Contribution of zooplankton nutrient recycling and effects on phytoplankton size structure in a hypereutrophic reservoir

Tyler J. Butts[1,3*], Eric K. Moody[2], Grace M. Wilkinson[1,3]

[1]Ecology, Evolution and Organismal Biology Department, Iowa State University, Ames, IA

[2]Department of Biology, Middlebury College, Middlebury, VT

[3]Current Address: Center for Limnology, University of Wisconsin – Madison, Madison, WI

***Corresponding Author:**

Tyler Butts

tjbutts@wisc.edu

Key Words: nutrient cycling, stoichiometry, hypereutrophic, body size, excretion

ABSTRACT

Consumer nutrient recycling influences aquatic ecosystem functioning by altering the movement and transformation of nutrients. In hypereutrophic reservoirs, zooplankton nutrient recycling has been considered negligible due to high concentrations of available nutrients. A comparative analysis (Moody and Wilkinson, 2019) found that zooplankton communities in hypereutrophic lakes are dominated by nitrogen (N)-rich species, which the authors hypothesized would increase phosphorus (P) availability through excretion. However, zooplankton nutrient recycling likely varies over the course of a growing season due to changes in biomass, community composition, and grazing pressure on phytoplankton. We quantified zooplankton, phytoplankton, and nutrient concentration dynamics during the summer of 2019 in a temperate, hypereutrophic reservoir. We found that the estimated contribution of zooplankton excretion to the dissolved nutrient pool on a given day was equivalent to a substantial proportion (21-39%) of the dissolved inorganic P standing stock in early summer when P concentrations were low and limiting phytoplankton growth. Further, we found evidence that zooplankton affected phytoplankton size distributions through selective grazing of smaller phytoplankton cells likely affecting nutrient uptake and storage by phytoplankton. Overall, our results demonstrate zooplankton excretion in hypereutrophic reservoirs likely helped drive springtime phytoplankton dynamics through nutrient recycling while grazing influenced phytoplankton size distributions.

INTRODUCTION

Animal consumers contribute to nutrient cycling in aquatic ecosystems by controlling the movement and transformation of nutrients over time and across space (Atkinson *et al.*, 2017). Aquatic consumers, like zooplankton, ingest phytoplankton then excrete and egest metabolized and unassimilated materials as waste, recycling nutrients back into the ecosystem (Vanni, 2002). Bioavailable nutrients are then taken up by phytoplankton to produce new biomass controlled by rates of nutrient uptake, cell size, and elemental stoichiometry (Finkel *et al.*, 2010; Sarnelle and Knapp, 2005). Imbalances between consumer demand for and assimilation efficiency of nutrients, as well as the elemental composition of phytoplankton, drives the stoichiometry of nutrients recycled back into the ecosystem (Elser and Hassett, 1994; Sterner, 1990). Consumer-resource imbalances lead to greater nutrient recycling of a particular element that may result in

changes to ecosystem nutrient limitation and alter trophic interactions between consumers and their resource (Elser *et al.*, 2000; Dobberfuhl and Elser, 2000).

The community composition of both phytoplankton and zooplankton can influence the stoichiometry of recycled nutrients and generate strong differences in nitrogen (N) and phosphorus (P) recycling (Balseiro *et al.*, 1997). For example, copepods and small cladocerans generally retain more N whereas *Daphnia* generally retain more P (Elser and Urabe, 1999). Differences in N and P retention between zooplankton taxa can result in copepod and small cladoceran-dominated communities retaining more N and recycling more P, potentially driving phytoplankton to N-limitation (Elser *et al.*, 2000, 1988). Further, differences in zooplankton preferred food size influence the species and morphology of phytoplankton subjected to grazing. For example, *Bosmina spp.* are moderately selective filter feeders, many copepods are highly selective raptorial feeders, and *Daphnia* are highly general filter feeders (Barnett *et al.*, 2007; *but see*, Hood and Sterner, 2010). Selection for phytoplankton based on zooplankton community grazing preferences and selectivity may then alter the phytoplankton community cell sizes and elemental composition ultimately influencing nutrient recycling (Finkel *et al.*, 2010). Phytoplankton community composition varies with trophic state, grazing pressure, and nutrient availability as different genera preferentially assimilate different forms of nitrogen (Andersen *et al.*, 2020). Cyanobacteria-dominated phytoplankton communities, which often arise in nutrient enriched ecosystems, are particularly resistant to zooplankton grazing due to the ability of many genera to form colonies or filaments, their poor nutritional quality, and toxin production (Moustaka-gouni and Sommer, 2020). During periods of cyanobacterial dominance, the majority of the zooplankton community can shift to grazing on smaller, unicellular phytoplankton that have different elemental stoichiometry and nutrient uptake rates (Beardall *et al.*, 2009). In combination, zooplankton-phytoplankton interactions affect nutrient recycling in aquatic ecosystems; however, the effects may vary depending on the severity of nutrient enrichment.

Much of our understanding regarding zooplankton nutrient recycling comes from oligotrophic and eutrophic ecosystems (Elser *et al.*, 2000; Moegenburg and Vanni, 1991), though many temperate lakes and reservoirs are increasingly becoming hypereutrophic due to continued land use conversion and climate change (Stoddard *et al.*, 2016). The extremely high nutrient concentrations in hypereutrophic reservoirs can produce unique conditions compared to less enriched waterbodies such as large seasonal variability in nutrient limitation of phytoplankton

growth (Andersen *et al.*, 2020), substantial internal P loading under oxic and anoxic conditions (Albright and Wilkinson, 2022; Song and Burgin, 2017), and a more complex mix of top-down and bottom-up forces affecting phytoplankton communities (Matsuzaki *et al.*, 2018). However, the contribution of zooplankton nutrient recycling in hypereutrophic ecosystems is often considered less important than other consumers like fish which can reach higher biomass in nutrient-rich ecosystems (Spooner *et al.*, 2013; Wilson and Xenopoulos, 2011; Vanni *et al.*, 2006). Despite this, zooplankton may still influence nutrient availability in hypereutrophic reservoirs as nutrient limitation and zooplankton biomass shift throughout the growing season. Additionally, selective feeding on small phytoplankton by small-bodied zooplankton can increase the dominance of large phytoplankton species, including filamentous and colonial cyanobacteria (Erdoğan *et al.*, 2021). This shift may influence nutrient availability as cyanobacteria have the capacity for luxury nutrient uptake, subsequent storage of excess nutrients, and the ability of some to fix atmospheric N (Cottingham *et al.*, 2015). As hypereutrophic lakes and reservoirs are often dominated by smaller-bodied zooplankton including microzooplankton and ciliates, selective grazing pressure on the phytoplankton community may indirectly influence nutrient availability.

A recent analysis of mesozooplankton (i.e., copepods, cladocerans, and rotifers; hereafter zooplankton) stoichiometric traits found that community N:P ratios shifted towards N-rich species with increasing eutrophication (Moody and Wilkinson, 2019). As such, in hypereutrophic ecosystems, zooplankton may contribute to P availability through recycling. This hypothesis was supported by the fact that the seston N:P was lower in hypereutrophic lakes and reservoirs compared to less-enriched ecosystems. This analysis suggested that the unique functioning of hypereutrophic lakes and reservoirs, even compared to eutrophic ecosystems, was due in part to the consumers inhabiting them. However, this was a comparative study among many lakes and reservoirs based on a single sampling point in the late summer. It is well established that zooplankton and phytoplankton communities are dynamic and undergo a seasonal succession during the summer driven by both top-down and bottom-up processes, which can vary depending on trophic state and other variables (Sommer *et al.*, 2012). Furthermore, the balance of top-down and bottom-up forces in lakes and reservoirs varies with nutrient ratios and concentrations across a season (Rogers *et al.*, 2020). In the scope of this comparative study (Moody and Wilkinson, 2019), the seasonal variability within zooplankton, phytoplankton, and nutrient dynamics was

not captured. As such, it remains unclear how nutrient availability and phytoplankton communities are influenced by nutrient recycling and top-down grazing throughout the summer in hypereutrophic ecosystems.

We investigated the role of zooplankton nutrient recycling and top-down grazing on nutrient availability, phytoplankton biomass, and community composition in a hypereutrophic reservoir across a summer growing season. Specifically, our objectives were to (1) evaluate the temporal dynamics and magnitude of the contribution of zooplankton body nutrient storage and excretion to nutrient availability and (2) assess the effect of zooplankton grazing on phytoplankton biomass, community composition, and size structure over the growing season. To estimate the storage and flux of nutrients driven by zooplankton consumers we used effect traits that link individual body size and elemental composition to ecosystem processes (Hébert *et al.*, 2017; Hébert *et al.*, 2016b). We hypothesized that zooplankton excretion would contribute most substantially to P availability early in the growing season due to higher zooplankton biomass in the spring (Sommer et al. 2012), low zooplankton community P storage, and lower rates of internal loading during this period. Conversely, we expected the contribution of zooplankton to N availability would be low at this time with high external loading of N from the watershed in the spring. We also hypothesized that zooplankton grazing, varying with community composition over the summer, would affect phytoplankton size structure due to selective grazing on smaller phytoplankton as well as drive changes in phytoplankton community composition. As such, smaller zooplankton body size would be associated with larger individual phytoplankton cell, colony, or filament sizes.

METHODS

Study Lake

Green Valley Lake (46°06’02” N, 94°23’05” W) is a hypereutrophic reservoir built in 1952 as an impoundment of the Platte River in southwestern Iowa (USA). The maximum depth is 7.3 m, with an average depth of 3.2 m and a surface area of 156 ha. Crappie (*Pomoxis spp.),* bluegill (*Lepomis macrochirus*), and largemouth bass (*Micropterus salmoides*) dominate the fish community. Additionally, there is a small population of common carp (*Cyprinus carpio*) and channel catfish (*Ictalurus punctatus*) (IDNR, 2022). The watershed is dominated by row crop agriculture (68.4% corn/soybean rotation). Consequently, Green Valley Lake is enriched with

nutrients and beset by annual phytoplankton blooms dominated by cyanobacteria (Supplementary Figure S1). To characterize zooplankton nutrient recycling in Green Valley Lake, we sampled zooplankton, phytoplankton, and nutrient concentrations weekly at the deepest point in the reservoir from early May (day of year; DOY 143) to early September (DOY 251) of 2019. We sampled again on DOY 273, but only collected zooplankton and nutrient samples at that time. Additionally, we deployed a YSI EXO3 sonde (Yellow Springs Instruments, Yellow Springs, Ohio, USA) at 0.5 m at the deepest point in the reservoir and collected temperature and pH measurements every 15 minutes. We used daily averages for the dates sampled of each variable in our analyses.

Nutrient Measurements

The concentration and form of nutrients in Green Valley Lake were measured throughout the growing season to compare to the magnitude and temporal dynamics of zooplankton excretion (objective 1) and to assess the drivers of phytoplankton biomass and community composition (objective 2). We collected surface water samples at a depth of 0.25 m at the deep point. We filtered a subset of the water sample through Whatman glass fiber filters (pore size = 0.45 µm) in the field, preserved with concentrated sulfuric acid to a pH of 2, and stored at 4 ºC until later analysis for soluble reactive phosphorus (SRP) and nitrate + nitrite (NOx). Ammonium is rarely detectable in Green Valley Lake during the summer (see Supplementary Material) and was therefore not measured for our study. We preserved unfiltered sample water with concentrated sulfuric acid to a pH of 2 and stored at 4 ºC until later analysis for total phosphorus (TP) and total nitrogen (TN). We used the ascorbic acid method to quantify P concentrations with filtered water for SRP and unfiltered water that had undergone persulfate digestion for TP. We used second-derivative ultraviolet spectroscopy to quantify NOx concentrations in filtered samples and TN concentrations following persulfate digestion. The N species were analyzed using an Agilent Cary 8454 UV-VIS spectrophotometer (Agilent Technologies Inc, Santa Clara, CA, USA) and analyzed P species using a Seal Analytical AQ2 Discrete Analyzer (Seal Analytical Inc. Mequon, WI, USA). For data analysis, nutrient concentrations below the limit of detection were replaced with the instrument-specific long-term method detection limit.

The nutrient concentrations were used to calculate total and dissolved inorganic molar N:P ratios. Nutrient limitation of phytoplankton growth was estimated based on the molar TN:TP ratio with N:P > 20 indicating P limitation (Guildford and Hecky, 2000).

Plankton Measurements

For each sampling event, zooplankton biomass and community composition were quantified to estimate the magnitude of nutrient excretion as well as the stoichiometry of nutrient storage (objective 1). In addition, phytoplankton biomass and community composition were quantified to compare with zooplankton dynamics across the summer growing season. Phytoplankton size structure and community composition were quantified to assess the temporal dynamics of zooplankton grazing (objective 2). Zooplankton were sampled via a vertical tow of a Wisconsin net (63 µm mesh) from 6 m depth. The samples were preserved with a formaldehyde solution (5% concentration after sample addition) in the field and later transferred to 70% ethanol. Phytoplankton samples were a composite sample over depth. We collected water in a 4 L Van Dorn sampler from 0.25, 1, 2, 3, and 4 m depths (the top of the thermocline), then mixed it in a 20 L carboy in the field. We then took a 1 L sample from the carboy following thorough mixing and preserved with Lugol's solution in the field.

We identified and enumerated zooplankton samples with a Leica MZ8 stereomicroscope connected to Motic Images software. For each sample, a 1 mL subsample was taken and a minimum of 60 individual zooplankton were identified to genus for cladocerans and rotifers, order for copepods, and class for ostracods. Copepod nauplii could not be identified to order and were simply identified as nauplii. If less than 60 organisms were in the subsample, we counted a second 1 mL subsample. We measured zooplankton lengths for up to 25 individuals per taxon per sample to calculate dry mass per liter using length-mass regressions (McCauley, 1984; Dumont *et al.*, 1975). For visual display of the zooplankton data, they were separated into nine taxonomic groups: *Daphnia, Simocephalus, Ceriodaphnia*, *Bosmina, Chydorus*, rotifers, calanoids, cyclopoids, nauplii, and ostracods (Supplementary Table S1). *Simocephalus* contributed only 7% of total community biomass at its peak and so were grouped with *Daphnia* for further statistical analyses.

We transferred the 1 L phytoplankton samples to a graduated cylinder and allowed phytoplankton to settle in a dark environment for 8 days before removing the supernatant with a

vacuum pump, leaving 50 mL of concentrated sample. We then removed a subsample from the concentrated sample and identified and enumerated individuals using a modified Palmer-Maloney chamber. We identified phytoplankton to genus and measured them using a calibrated ocular reticle on a Leitz DM IL inverted microscope at 400x magnification. For each sample, we measured a minimum of 300 natural units across 8 fields. We calculated biovolume per liter based on phytoplankton shape and then converted to wet biomass per liter assuming a 1:1 ratio between wet mass and biovolume (Hillebrand *et al.*, 1999; Sournia, 1978). We also measured the greatest axial linear dimension (GALD) of phytoplankton as the greatest distance across an individual cell, colony, or filament (i.e., natural unit), such as would be encountered by a zooplankton grazer. Like zooplankton, we separated phytoplankton genera into six groups for visual display: bacillariophytes, chlorophytes, chryso- and cryptophytes, *Aphanothece*, *Microcystis*, and other cyanophytes (Supplementary Table S2). Both *Aphanothece* and *Microcystis* were the dominant genera of cyanobacteria, contributing the majority of phytoplankton biomass (88 ± 18%; s.d.) and therefore were visualized separately.

Zooplankton Stoichiometry and Excretion Analysis

To assess the contribution of zooplankton excretion to nutrient availability (objective 1) we calculated zooplankton community elemental composition, nutrient storage, and excretion rate. We estimated elemental composition and total nutrient storage by zooplankton (L^{-1} d^{-1}) following methods described previously (Moody and Wilkinson, 2019). Briefly, we used taxa-specific %N and %P information collected from the literature (Hamre, 2016; Hébert *et al.*, 2016a; Hessen *et al.*, 2007) to estimate total nutrient storage by multiplying %N and %P by the biomass of each taxa and summing across the community on each sampling date. Although we are using trait data from largely oligotrophic lakes, zooplankton have fairly strong stoichiometric homeostasis (Persson *et al.*, 2010) as well as low intraspecific stoichiometric variation between aquatic ecosystems (Prater *et al.*, 2017) and variable food quality (Teurlincx *et al.*, 2017). Thus, it is unlikely that intraspecific variation in %N and %P have a large influence on our calculations.

We estimated excretion rates of N and P by zooplankton using published allometric equations (Supplementary Material). The equations relate zooplankton body size to N (ammonia) and P (phosphate) derived from a compiled dataset of marine and freshwater zooplankton species

(Hébert *et al.*, 2016b, 2016a). Temperature is an important control on an organism's metabolism, however, the excretion rates used to calculate the allometric equations accounted for differences in temperature by applying a standardized temperature correction (Hébert *et al.*, 2016a; Hernández-León and Ikeda, 2005). Therefore, the temperature dependence of metabolism and excretion is not being incorporated into the seasonal aspect of our study. Additionally, the allometric equations were not derived using data from rotifers, but rather for copepods and cladocerans. As such, we removed rotifers from our excretion analyses. For each sampling event, we used the average dry mass of each zooplankton taxon present to calculate individual N and P excretion rates (μM N or P individual^{-1} hour^{-1}) using the allometric equations. We then converted the hourly excretion rate to a daily rate (day^{-1}) and multiplied the daily rate by the density of each taxon (individuals L^{-1}) to calculate the taxon-specific daily excretion rates. Finally, we summed the daily excretion rates across all taxa on a sampling date to calculate the total zooplankton community excretion rate (μM N or P day^{-1}). Uncertainty in the excretion estimates was calculated by propagating the variation in the slope and intercept from the allometric equations presented in Hébert *et al.*, (2016b) through our calculations of the community excretion rates. Given that these calculations are an estimate, we also calculated zooplankton excretion using other published allometric equations from Wen and Peters (1994) derived from different underlying datasets. The overall pattern of zooplankton excretion did not differ between the two methods; however, the Wen and Peters (1994) based estimates of excretion were slightly higher (Supplementary Table S3). We chose to use the more conservative estimate of zooplankton excretion rates based on Hébert et al. (2016) in our analysis as the available information also allowed us to estimate uncertainty.

To assess the magnitude of zooplankton N and P excretion in Green Valley Lake we compared the estimated concentration of excreted N and P over the course of a day to the measured surface water concentrations of dissolved inorganic N and P for each sampling event, assuming diel nutrient concentrations remain relatively stable over 24 hours (Shirokova *et al.*, 2020; Nimick *et al.*, 2011). We expressed this value as a percent of the dissolved inorganic nutrient pool:

$$\left(\frac{\mu M\ N\ or\ P\ excreted\ by\ zooplankton\ community\ in\ a\ day}{\mu M\ of\ inorganic\ N\ or\ P\ present\ in\ the\ surface\ waters}\right) * 100 \qquad (1)$$

To assess how zooplankton excretion would affect nutrient cycling over the course of the growing season we calculated the zooplankton nutrient turnover time of the dissolved inorganic P pool (Conroy *et al.*, 2005). Zooplankton nutrient turnover time relates to nutrient cycling by estimating the number of days it would take for zooplankton excretion to replenish the mass of P (the standing stock) measured in the reservoir on a given day independent of nutrient uptake. The turnover time varies depending on the rate of zooplankton excretion and concentration of inorganic dissolved P in the surface waters. Short turnover times indicate zooplankton are contributing substantially to the dissolved inorganic P pool in Green Valley Lake. Long turnover times indicate factors other than zooplankton excretion are driving nutrient availability.

Zooplankton Grazing and Phytoplankton Size Structure Analysis

To assess the effect of zooplankton grazing on phytoplankton size structure and community composition (objective 2) we estimated the relative strength of top-down v. bottom up-control, compared zooplankton and phytoplankton size distributions, estimated zooplankton feeding range, and assessed the drivers of phytoplankton community composition across the growing season in Green Valley Lake. We determined the relative importance of top-down v. bottom-up control in lakes by calculating the ratio (expressed as a percentage of zooplankton biomass relative to phytoplankton biomass (Filstrup *et al.*, 2014; Heathcote *et al.*, 2016). A high zooplankton to phytoplankton biomass percentage (~40-50%) indicates strong top-down control, whereas a low percentage (~10%) indicates weak top-down control (Leroux and Loreau, 2015; Havens and Beaver, 2013). Additionally, we compared the size distributions of zooplankton and phytoplankton communities over time using our measurements of zooplankton length and phytoplankton GALD. Phytoplankton sizes span orders of magnitudes and are selected for by diverse pressures, thus the distribution of phytoplankton GALD can be used to infer nutrient uptake and grazing pressure (Litchman *et al.*, 2010). We compared distributions of zooplankton length and body mass to the distribution of phytoplankton GALD for each sampling date to investigate the size distribution dynamics over time. Additionally, we performed a Pearson correlation of mean phytoplankton GALD versus mean zooplankton size to assess whether phytoplankton GALD was dictated by zooplankton body size.

In addition to zooplankton body size, functional feeding groups can affect how zooplankton interact with phytoplankton, either through selective raptorial feeding or non-

discriminate grazing (Barnett *et al.*, 2007). We collected data from the literature on food size range, the smallest and largest reported particles consumed by a taxa, based on constituents of the zooplankton community on each sample date. We then incorporated the zooplankton community food size range into our comparison of zooplankton and phytoplankton size distributions (Supplementary Material). Briefly, we compiled the minimum and maximum reported food size range for groups of taxa we observed within our study (Supplementary Table S4). We then calculated a daily mean minimum and maximum food size range for the zooplankton community weighted by taxon biomass. The effective food size range was then compared to the distributions of zooplankton length and phytoplankton GALD. To assess the drivers of phytoplankton community composition across the growing season we performed a distance based-redundancy analysis (db-RDA). We included potentially important environmental variables such as dissolved inorganic nutrient concentrations (Filstrup and Downing, 2017), temperature (Striebel *et al.*, 2016)**,** and pH (Rönicke *et al.*, 2010), as well as zooplankton biomass, excretion N:P, and body stoichiometry (Table 1**).** We used a Hellinger transformation for the phytoplankton genera biomass data and removed genera that only occurred once in the full dataset and contributed <1% of total biomass to decrease the weight of rare species. Environmental variables were z-transformed in order to correct for differences in scale and magnitude (Legendre and Legendre, 1998). We performed the db-RDA using a Bray-Curtis distance matrix taking the square root of dissimilarities to avoid negative eigenvalues (Legendre and Anderson, 1999). We removed missing or lost samples from the final analysis. Forward and backward stepwise regression was used to select the best model. We determined model significance using a Monte Carlo permutation test (999 permutations, p-value < 0.05). We then confirmed the variables used in the final model did not contain any multicollinearity by ensuring the square root of each variable's variance inflation factor was less than two.

All analyses were performed using the statistical software R version 4.0.4 (R Core Team, 2021) with the, *magrittr*, and *vegan* packages (Bach and Wickham, 2020; Oksanen *et al.*, 2020).

RESULTS

Seasonal Dynamics

Nutrient concentrations and inferred limitation of phytoplankton growth were dynamic throughout the summer (Figure 1). Dissolved inorganic N concentrations were highest in the

spring and decreased by 80% from the peak after DOY 178 (Figure 1A). At the same time, there was a rapid increase in dissolved inorganic P by 394% from DOY 172 to 178 and a 937% increase from DOY 178 to DOY 206 (Figure 1B). Molar TN:TP declined rapidly in mid-July (DOY 192), transitioning the ecosystem from P- to intermittent N-limitation. There was also a shift in dissolved inorganic N:P to N-limitation in mid-July that was persistent for the remainder of the summer (Figure 1C). Zooplankton elemental body composition was dominated by N storage in both the early and late summer. Zooplankton P storage remained relatively low, but nearly equaled dissolved inorganic P concentrations in the water column early in the summer (Figure 1B). Zooplankton community body N:P was quite variable with the highest N:P ratios in early to mid-summer and relatively low values near the end of summer (Figure 1D). However, the increases in dissolved inorganic P observed in the water column were not concurrent with increases in zooplankton community body N:P and instead were likely driven by other processes in the lake.

Zooplankton and phytoplankton biomass and community composition varied substantially over the summer growing season. Zooplankton biomass peaked at 249 µg L^{-1} in late May and early June (DOY 150-164), rapidly decreased (~2 µg L^{-1}) in mid-July to late August (DOY 192 – DOY 234), before increasing in early autumn (Figure 2A). The early summer zooplankton community was dominated by *Daphnia* and calanoid copepods which transitioned in early July (DOY 199) to *Chydorus* and cyclopoid copepods, before transitioning back to *Daphnia* in late August (Figure 2A). Similarly, phytoplankton biomass was initially high in the spring, mainly composed of bacillariophytes, before rapidly decreasing during the clear-water period between DOY 150 – 164 (Figure 2B). Following DOY 172, the phytoplankton community was overwhelmingly composed of cyanophytes, mainly *Microcystis*, with phytoplankton reaching peak biomass on DOY 213 (~329 mg L^{-1}). *Daphnia* biomass decreased rapidly following increasing *Microcystis* biomass coinciding with an overall decrease in zooplankton biomass (Figure 2). The other abundant cyanophyte was the diazotroph *Aphanothece,* which was present from DOY 192 – 228.

Zooplankton Excretion

The daily estimated concentration of P excreted by zooplankton was equivalent to a substantial portion of the dissolved inorganic P pool. However, this contribution was only

particularly large from late May to late June (DOY 143-172). The concentration of daily excretion during this early summer period was between 21-39% of the dissolved inorganic P standing stock (Figure 3A). This proportionally high contribution from zooplankton P excretion coincided with a period of higher zooplankton body N:P (Figure 1D) and higher zooplankton body N storage. Following DOY 172, the concentration of P excreted by zooplankton dropped below 1% of the dissolved inorganic P pool for the remainder of the sampling period. Zooplankton excretion contributed to a rapid turnover of the dissolved inorganic P pool in early summer with turnover times ranging between 3 – 5 days but increased beyond 200 days as dissolved inorganic P concentrations increased in late June (Supplementary Table S5). Estimated zooplankton N excretion was never equivalent to more than 3.3% of the dissolved inorganic N pool (Figure 3B). The N:P ratio of zooplankton excretion was relatively stable over the course of the growing season (Supplementary Figure S2).

Plankton Size Structure

The ratio of zooplankton: phytoplankton biomass was less than 7% throughout the summer, indicating minimal top-down control on phytoplankton biomass (Supplementary Figure S3). However, based on the plankton size distributions, zooplankton likely influenced phytoplankton GALD in mid- to late summer. Small zooplankton dominated from late June to early August (DOY 178 – 213) concurrent with a period in which larger phytoplankton dominated the GALD distribution (Figure 4A). Phytoplankton average GALD was greatest in July (mean = 32.5 ± 19.6 µm; s.d.) when zooplankton average length was at its lowest (mean = 171 ± 102 µm; s.d.). During this period (DOY 192 – 199) the zooplankton community food size range included 0 - 3% of individual phytoplankton GALD measurements, which were the lowest percentages of the entire growing season (Supplementary Figure S4). We also found evidence that smaller zooplankton body size was associated with larger phytoplankton GALD supporting our prediction**.** In late July through August, the difference in zooplankton length and phytoplankton GALD steadily increased, surpassing the mean differences observed in early summer (Figure 4B). A similar pattern was observed between phytoplankton GALD and zooplankton dry mass (Supplementary Figure S5). Additionally, there was a weak negative correlation between GALD and zooplankton length (p=0.0119, r(12)=-0.65; Supplementary Figure S6A), and zooplankton body mass (p=0.0306, r(12)=-0.58; Supplementary Figure S6B).

Contrary to our hypothesis, the db-RDA analysis showed that variation in phytoplankton community composition was not significantly influenced by zooplankton (Figure 5, Table 2). Following variable selection and removal of multicollinear variables only dissolved inorganic N (p=0.043) and temperature (p=0.003) were significantly correlated with variation in phytoplankton community composition explaining 21.9% of total variation. Additionally, only the first axis was significant which separated the phytoplankton community between pre- and post-dominance of cyanobacteria (F=3.62, p=0.004). Phytoplankton community composition was correlated with dissolved inorganic N in early summer prior to the cyanobacteria bloom. Beginning on DOY 172 phytoplankton community composition became more correlated with temperature.

DISCUSSION

We sought to better understand zooplankton nutrient cycling in hypereutrophic ecosystems by observing zooplankton-phytoplankton dynamics and nutrient concentrations across a summer growing season. We used size and stoichiometric traits to infer excretion and body stoichiometry to assess the degree to which zooplankton influenced the transformation and flux of nutrients within the water column despite the high variability observed in these pools over time. We found that zooplankton excretion contributed substantially to P availability during the early summer, potentially having a bottom-up effect on phytoplankton biomass (objective 1). In late summer, we found zooplankton size structure likely influenced phytoplankton community size structure with smaller-bodied zooplankton having a top-down effect, resulting in increased phytoplankton GALD (objective 2). However, contrary to our hypothesis, we found that zooplankton did not influence phytoplankton community composition.

Nutrient and Plankton Seasonal Dynamics

The seasonal transition between P and N-limitation or co-limitation we observed in Green Valley Lake has also been reported in other eutrophic and hypereutrophic ecosystems (Andersen *et al.*, 2020; Wang *et al.*, 2019). In Green Valley, the large increase in dissolved inorganic P beginning on DOY 178 resulted in the transition from strong P-limitation to co-limitation or N-limitation. This increase in dissolved P in the surface waters was driven by both oxic and anoxic internal P loading (Albright and Wilkinson, 2022). Zooplankton and phytoplankton biomass and

community composition were quite variable, though they both roughly followed expected patterns of seasonal succession (Sommer *et al.* 2012).

Effect of zooplankton excretion on nutrient availability

Supporting our first hypothesis, we found that zooplankton excretion of P was equivalent to a large portion (21 – 39%) of the dissolved inorganic P pool in Green Valley Lake, but only during early summer (objective 1). It was during this period that dissolved inorganic P was at relatively low concentrations in the water column (0.13 – 0.19 µM) and phytoplankton growth was likely P-limited, indicating that zooplankton-mediated recycling contributed to meeting nutrient demand by phytoplankton during this time. This early-season P availability, facilitated by zooplankton recycling, may have helped initialize the cyanotoxin-producing cyanobacteria bloom that flourished later in the season and persisted until late summer (Isles and Pomati, 2021). The contribution of zooplankton excretion to dissolved inorganic P availability is consistent with the hypothesis from Moody and Wilkinson (2019) that N-rich zooplankton communities can contribute to increased P availability within nutrient-rich ecosystems. However, we found that zooplankton community N:P and zooplankton excretion dynamics were context- and time-dependent over the course of the growing season. As such, zooplankton-mediated flux of P was mainly confined to the early part of the growing season when zooplankton biomass was high, zooplankton community N-storage was relatively high, and dissolved inorganic P concentrations were relatively low. Furthermore, our estimates of P turnover by zooplankton indicated rapid turnover of dissolved inorganic P during early summer, but turnover drastically slowed once P concentrations rose. These results support our conclusions that zooplankton nutrient recycling was an important P flux during the early summer growing season, but not an important flux once internal loading increased P availability.

Overall, the contribution of zooplankton nutrient-recycling to the dissolved inorganic N pool in Green Valley Lake was negligible. However, the uptake of ammonium from zooplankton excretion by phytoplankton may have been too fast to result in a measurable concentration, masking the contribution of zooplankton excretion to N availability. Alternatively, we may be underestimating N excretion given that our estimates of zooplankton excretion were not taxon-specific, but instead based on a consolidated dataset of both cladocerans and copepods. This is particularly true when daphniids dominate in the early and late-summer periods, which could

increase community N excretion as *Daphnia* retain more P than N due largely to their body stoichiometry (Elser *et al.*, 1988). Overall, our estimates of zooplankton excretion were low relative to the concentrations of dissolved inorganic nutrients in the ecosystem across the summer; however, they were comparable with other studies using similar allometric equations (Conroy *et al.*, 2005) or direct measurement (den Oude and Gulati, 1988) in eutrophic ecosystems. The low variability in zooplankton excretion N:P was likely an artifact of the allometric equations we used to estimate excretion. The excretion estimates used to build the allometric equations were derived from a combination of copepod and cladoceran species in both freshwater and marine environments. This collation of multiple species likely masked any variation in excretion N:P we would expect to observe from differences in food quality and species elemental composition.

In addition to zooplankton, other consumers can play a key role in nutrient recycling in eutrophic lakes and reservoirs, particularly detritivores and planktivores such as gizzard shad (Sharitt *et al.*, 2021; Vanni *et al.*, 2006) and mussels (Arnott and Vanni, 1996). However, neither gizzard shad nor zebra mussels have been reported in Green Valley Lake. While we did not quantify the contribution of nutrient recycling by other consumers to availability in Green Valley Lake, these organisms certainly contributed. There is a common carp (*Cyprinus carpio*) population in Green Valley Lake which can influence nutrient cycling through bioturbation and excretion (Weber and Brown, 2009); however, the population is small. We hypothesize that the contributions of fish and other organisms would have a similar seasonality given the large contribution of internal P in the latter half of the season.

Role of zooplankton excretion and grazing on phytoplankton community structure

In support of our second hypothesis, we found evidence that zooplankton community size structure may have influenced the size structure of the phytoplankton community (objective 2). This is despite the fact that we observed weak top-down control on phytoplankton biomass, consistent with other studies in hypereutrophic lakes (Rogers *et al.*, 2020; Matsuzaki *et al.*, 2018). The negative correlation between zooplankton length and phytoplankton GALD is consistent with other studies in hypereutrophic ecosystems indicating that small-bodied zooplankton preferentially graze on smaller phytoplankton, increasing the dominance of large filamentous and colonial phytoplankton (Bairagi *et al.*, 2019; Onandia *et al.*, 2015). By grazing

on smaller sized phytoplankton cells or colonies, zooplankton can reduce the abundance of smaller phytoplankton leaving a greater proportion of individuals with large GALD to dominate the overall size distribution. This was evidenced by the phytoplankton community size structure shifting towards higher GALD, likely driven by an increase in *Microcystis* colonies observed in July through early August. It is likely that smaller-bodied zooplankton were contributing, in part, to the dominance of *Microcystis* colonies and higher phytoplankton GALD by removing smaller phytoplankton cells. The low percentage of phytoplankton GALD measurements that fell within the zooplankton community food size range midsummer suggests that zooplankton were grazing on smaller phytoplankton cells, increasing the average GALD of the phytoplankton community. Effectively, the phytoplankton left behind following zooplankton grazing were mostly large colonial *Microcystis.*

However, it is unlikely zooplankton were the sole cause of increased phytoplankton GALD. The drawdown of dissolved inorganic N we observed midsummer coincided with the bloom of *Microcystis* beginning on DOY 172, suggesting efficient N uptake by *Microcystis*. Availability of dissolved inorganic N promotes *Microcystis* growth and was likely influencing the proliferation of *Microcystis* colonies (Chen *et al.*, 2019). However, nutrients and grazing can interact to affect phytoplankton GALD, where grazing by zooplankton, along with increased nutrients, promotes greater phytoplankton community GALD (Cottingham, 1999). While *Microcystis* toxicity can dampen zooplankton grazing, zooplankton community grazing on toxic *Microcystis* has been documented previously (Davis et al. 2012). Furthermore, over the summer growing season, the increased incidence of toxin-producing Cyanobacteria can even induce shifts towards toxin-resistant phenotypes in zooplankton populations (Schaffner *et al.*, 2019). Thus, it is likely that zooplankton grazing on toxic cyanobacteria occurred in Green Valley Lake, influencing phytoplankton size structure. The size structure of communities is closely tied to food web structure and energy flow (Brose *et al.*, 2017), thus the influence of the zooplankton community on phytoplankton size structure we observed was likely influential on the transfer, uptake, and recycling of nutrients by phytoplankton.

It is also likely that microzooplankton and ciliates played an important role grazing on small phytoplankton species; however, we did not quantify these communities in this study. Furthermore, our phytoplankton counting methods were unable to facilitate the identification of nano- or picophytoplankton species in the water column. Microzooplankton, nano- and

picophytoplankton are increasingly recognized as key components of the plankton food web and contribute a significant percentage of grazing pressure on phytoplankton in highly productive ecosystems (Agasild *et al.*, 2007; Zingel *et al.*, 2007). Future studies should examine their seasonal dynamics and potential contribution to ecosystem processes more thoroughly as they can be key components of zooplankton-phytoplankton interactions in nutrient-rich reservoirs.

The redundancy analysis (db-RDA) suggested that neither zooplankton top-down control nor nutrient recycling significantly affected variation in phytoplankton community composition. The db-RDA was able to discriminate the phytoplankton community between pre- and post-cyanobacterial dominance likely driven by the overwhelming dominance of *Microcystis* beginning on DOY 172. The early summer phytoplankton community was significantly related to the concentration of dissolved inorganic N which corresponds with the seasonal dynamic of nutrient limitation we observed as both chlorophytes and bacillariophytes perform well under P-limitation (Berg *et al.*, 2003). Furthermore, the dissolved inorganic N pool was highest in early summer and predominantly composed of nitrate which can be taken up and used by bacillariophytes (Andersen *et al.*, 2020). The mid- to late-summer phytoplankton community was significantly related to temperature, consistent with other studies describing increasing temperature as a key driver of cyanobacteria dominance (Hayes *et al.*, 2020). Other unobserved environmental factors were likely influencing the phytoplankton community as the db-RDA described only 21.88% of variation in the phytoplankton community composition. Phytoplankton community turnover is a complex phenomenon driven by a multitude of environmental factors (Wentzky *et al.*, 2020; Sommer *et al.*, 2012), including nutrient and light availability, the latter of which we did not measure. Given the high biomass of phytoplankton, light limitation through self-shading likely played a significant role in phytoplankton dynamics.

CONCLUSIONS

While the importance of consumer-driven nutrient recycling has been demonstrated in less eutrophic waterbodies, the role that zooplankton consumers have on nutrient availability and phytoplankton dynamics in hypereutrophic reservoirs is understudied. Our results support a previous comparative study indicating that zooplankton community composition may influence nutrient availability in hypereutrophic ecosystems, as well as extend our understanding of the temporal dynamics of zooplankton and phytoplankton interactions. We found evidence of the

importance of zooplankton nutrient cycling in a hypereutrophic reservoir with zooplankton excretion providing a large portion of the available P early in the summer, prior to the onset of the cyanobacteria-dominated bloom later in the season. If we had only assessed the late summer period or only a few time points across the summer, we would have likely missed the important dynamics in nutrient availability and zooplankton nutrient cycling we observed. In addition to the bottom-up influences of zooplankton, we found that zooplankton affected phytoplankton size structure contributing to increased phytoplankton community GALD. While we did not observe total top-down control of the phytoplankton community, the influence of zooplankton on phytoplankton size structure has important implications to nutrient recycling as size is a key trait regulating biogeochemical cycling in phytoplankton. As demonstrated here, the role of zooplankton nutrient recycling in hypereutrophic reservoirs is an important component of phytoplankton dynamics and ecosystem function that should be considered in greater detail. Unlike previous assumptions that zooplankton do not contribute substantially to nutrient cycling and phytoplankton dynamics in hypereutrophic ecosystems, our results suggest that zooplankton do in fact contribute to those dynamics, predominantly for a short period early in the summer. Future work should investigate the dynamics of zooplankton nutrient recycling across different climate contexts and over longer time periods, including dynamics through winter and autumn.

ACKNOWLEDGEMENTS

We would like to thank Shania Walker, Halle Rosenboom, Quin Shingai, Rachel Fleck, Elena Sandry, Psalm Amos, Julia Schneller, Adriana Le-Compte, and Ellen Albright for assistance with sample collection and analysis. Additionally, we thank Riley Barbour for assistance with phytoplankton identification and enumeration. We thank Dr. Marie-Pier Hébert and one anonymous reviewer for providing insightful comments that improved the manuscript.

FUNDING

This project was funded by the Iowa Department of Natural Resources (Grant # 19CRDLWBMBALM-0010) and the U.S. Department of Agriculture National Institute of Food and Agriculture (Grant # 2018-09746)**.** This material is based upon work supported by the National Science Foundation (NSF) Graduate Research Fellowship Program (Grant # DGE-1747503) and NSF Grant # 2200391 to Wilkinson. Any opinions, findings, and conclusions or recommendations expressed in this material are those of the authors and do not necessarily reflect the views of the National Science Foundation.

DATA ARCHIVING

The data for this study will be archived using the Environmental Data Initiative repository and given a unique digital object identifier. Data will be uploaded in a comma delimited file format with metadata composed of contact information, detailed variable descriptions, complete taxonomic information, temporal resolution, and descriptions for a given variable when appropriate. Metadata will follow the ecological metadata language and be published under a creative commons license. Scripts for data analysis and figure generation will be available and maintained online through GitHub (https://github.com/tjbutts/hyper-plankton) and will eventually be published in Zenodo for long-term storage.

REFERENCES

Agasild, H. *et al.* (2007) Contribution of different zooplankton groups in grazing on phytoplankton in shallow eutrophic Lake Võrtsjärv (Estonia). *Hydrobiologia*, **584**, 167–177.

Albright, E. and Wilkinson, G. (2022) Sediment phosphorus composition controls hot spots and

592 hot moments of internal loading in a temperate reservoir. *EarthArxiv*.
593 Andersen, I. M. *et al.* (2020) Nitrate, ammonium, and phosphorus drive seasonal nutrient
594 limitation of chlorophytes, cyanobacteria, and diatoms in a hyper-eutrophic reservoir.
595 *Limnol. Oceanogr.*, **65**, 962–978.
596 Arnott, D. L. and Vanni, M. J. (1996) Nitrogen and phosphorus recycling by the zebra mussel
597 (*Dreissena polymorpha*) in the western basin of Lake Erie. *Can. J. Fish. Aquat. Sci.*, **53**,
598 646–659.
599 Atkinson, C. L. *et al.* (2017) Consumer-driven nutrient dynamics in freshwater ecosystems: from
600 individuals to ecosystems. *Biol. Rev.*, **92**, 2003–2023.
601 Bach, S. and Wickham, H. (2020) magrittr: A forward-Pipe Operator for R.
602 Bairagi, N. *et al.* (2019) Zooplankton selectivity and nutritional value of phytoplankton
603 influences a rich variety of dynamics in a plankton population model. *Phys. Rev. E*, **99**,
604 012406.
605 Balseiro, E. G. *et al.* (1997) Nutrient recycling and shifts in N:P ratio by different zooplankton
606 structures in a South Andes Lake. *J. Plankton Res.*, **19**, 805–817.
607 Barnett, A. J. *et al.* (2007) Functional diversity of crustacean zooplankton communities : towards
608 a trait-based classification. 796–813.
609 Beardall, J. *et al.* (2009) Allometry and stoichiometry of unicellular, colonial and multicellular
610 phytoplankton. *New Phytol.*, **181**, 295–309.
611 Berg, G. M. *et al.* (2003) Plankton community composition in relation to availability and uptake
612 of oxidized and reduced nitrogen. *Aquat. Microb. Ecol.*, **30**, 263–274.
613 Brose, U. *et al.* (2017) Predicting the consequences of species loss using size-structured
614 biodiversity approaches. *Biol. Rev.*, **92**, 684–697.
615 Chen, Q. *et al.* (2019) Physiological effects of nitrate, ammonium, and urea on the growth and
616 microcystins contamination of Microcystis aeruginosa: Implication for nitrogen mitigation.
617 *Water Res.*, **163**, 114890.
618 Conroy, J. D. *et al.* (2005) Soluble nitrogen and phosphorus excretion of exotic freshwater
619 mussels (Dreissena spp.): Potential impacts for nutrient remineralisation in western Lake
620 Erie. *Freshw. Biol.*, **50**, 1146–1162.
621 Cottingham, K. L. *et al.* (2015) Cyanobacteria as biological drivers of lake nitrogen and
622 phosphorus cycling. *Ecosphere*, **6**, 1–19.

623 Cottingham, K. L. (1999) Nutrients and zooplankton as multiple stressors of phytoplankton
624 communities: Evidence from size structure. *Limnol. Oceanogr.*, **44**, 810–827.
625 Dobberfuhl, D. R. and Elser, J. J. (2000) Elemental stoichiometry of lower food web components
626 in arctic and temperate lakes. *J. Plankton Res.*, **22**, 1341–1354.
627 Dumont, H. J. *et al.* (1975) The dry weight estimate of biomass in a selection of Cladocera,
628 Copepoda and Rotifera from the plankton, periphyton and benthos of continental waters.
629 *Oecologia*, **19**, 75–97.
630 Elser, J. and Hassett, R. (1994) A stoichiometric analysis of the zooplankton-phytoplankton
631 interaction in marine and freshwater ecosystems. *Nature*, **370**, 211–213.
632 Elser, J. J. *et al.* (2000) Pelagic C:N:P Stoichiometry in a Eutrophied Lake: Responses to a
633 Whole-Lake Food-Web Manipulation. *Ecosystems*, **3**, 293–307.
634 Elser, J. J. *et al.* (1988) Zooplankton-mediated transitions between N- and P-limited growth.
635 *Limnol. Oceanogr.*, **33**, 1–14.
636 Elser, J. and Urabe, J. (1999) The Stoichiometry of Consumer-Driven Nutrient Recycling:
637 Theory, Observations, and Consequences. *Ecology*, **80**, 735–751.
638 Erdoğan, Ş. *et al.* (2021) Determinants of phytoplankton size structure in warm, shallow lakes. *J.*
639 *Plankton Res.*, **43**, 353–366.
640 Filstrup, C. T. *et al.* (2014) Cyanobacteria dominance influences resource use efficiency and
641 community turnover in phytoplankton and zooplankton communities. *Ecol. Lett.*, **17**, 464–
642 474.
643 Filstrup, C. T. and Downing, J. A. (2017) Relationship of chlorophyll to phosphorus and nitrogen
644 in nutrient-rich lakes. *Inl. Waters*, **7**, 385–400.
645 Finkel, Z. V. *et al.* (2010) Phytoplankton in a changing world: Cell size and elemental
646 stoichiometry. *J. Plankton Res.*, **32**, 119–137.
647 Guildford, S. J. and Hecky, R. E. (2000) Total nitrogen, total phosphorus, and nutrient limitation
648 in lakes and oceans: Is there a common relationship? *Limnol. Oceanogr.*, **45**, 1213–1223.
649 Hamre, K. (2016) Nutrient profiles of rotifers (Brachionus sp.) and rotifer diets from four
650 different marine fish hatcheries. *Aquaculture*, **450**, 136–142.
651 Havens, K. E. and Beaver, J. R. (2013) Zooplankton to phytoplankton biomass ratios in shallow
652 Florida lakes: An evaluation of seasonality and hypotheses about factors controlling
653 variability. *Hydrobiologia*, **703**, 177–187.

654 Hayes, N. M. *et al.* (2020) Effects of lake warming on the seasonal risk of toxic cyanobacteria
655 exposure. *Limnol. Oceanogr. Lett.*, **5**, 393–402.
656 Heathcote, A. J. *et al.* (2016) Biomass pyramids in lake plankton: influence of Cyanobacteria
657 size and abundance. *Inl. Waters*, **6**, 250–257.
658 Hébert, M. P. *et al.* (2016a) A compilation of quantitative functional traits for marine and
659 freshwater crustacean zooplankton. *Ecology*, **97**, 1081.
660 Hébert, M. P. *et al.* (2016b) A meta-analysis of zooplankton functional traits influencing
661 ecosystem function. *Ecology*, **97**, 1069–1080.
662 Hébert, M. P. *et al.* (2017) Linking zooplankton communities to ecosystem functioning: Toward
663 an effect-Trait framework. *J. Plankton Res.*, **39**, 3–12.
664 Hernández-León, S. and Ikeda, T. (2005) Zooplankton respiration. In del Giorgio, P. A. and le B.
665 Williams, P. (eds), *Respiration in aquatic ecosystems*. Oxford University Press, Oxford
666 (UK), p. 582.
667 Hessen, D. O. *et al.* (2007) RNA responses to N- and P-limitation; reciprocal regulation of
668 stoichiometry and growth rate in Brachionus. *Funct. Ecol.*, **21**, 956–962.
669 Hillebrand, H. *et al.* (1999) Biovolume calculation for pelagic and benthic microalgae. *J.*
670 *Phycol.*, **35**, 403–424.
671 Hood, J. M. and Sterner, R. W. (2010) Diet mixing: Do animals integrate growth or resources
672 across temporal heterogeneity? *Am. Nat.*, **176**, 651–663.
673 Iowa Department of Natural Resources (IDNR) (2022) Fish Survey Data.
674 https://www.iowadnr.gov/Fishing/Fish-Survey-Data
675 Isles, P. D. F. and Pomati, F. (2021) An operational framework for defining and forecasting
676 phytoplankton blooms. *Front. Ecol. Environ.*, in press.
677 Legendre, P. and Anderson, M. (1999) Distance-based redundancy analysis: Testing multispecies
678 responses in multifactorial ecological experiments. *Ecol. Monogr.*, **69**, 1–24.
679 Legendre, P. and Legendre, L. (1998) *Numerical Ecology*. 2nd ed. Elsevier, Amsterdam.
680 Leroux, S. and Loreau, M. (2015) Theoretical perspectives on bottom-up and top-down
681 interactions across ecosystems. In Hanley, T. and La Pierre, K. (eds), *Trophic Ecology:*
682 *Bottom-up and top-down interactions across aquatic and terrestrial systems*. Cambridge
683 University Press, pp. 3–27.
684 Litchman, E. *et al.* (2010) Linking traits to species diversity and community structure in

phytoplankton. *Hydrobiologia*, **653**, 15–28.
Matsuzaki, S. ichiro S. *et al.* (2018) Bottom-up linkages between primary production, zooplankton, and fish in a shallow, hypereutrophic lake. *Ecology*, **99**, 2025–2036.
McCauley, E. (1984) The estimation of the abundance and biomass of zooplankton in samples. In Downing, J. and Rigler, F. (eds), *A manual on methods for the assessment of secondary productivity in fresh waters*. Blackwell Publishing Ltd, Oxford (UK), pp. 228–265.
Moegenburg, S. M. and Vanni, M. J. (1991) Nutrient regeneration by zooplankton: Effects on nutrient limitation of phytoplankton in a eutrophic lake. *J. Plankton Res.*, **13**, 573–588.
Moody, E. K. and Wilkinson, G. M. (2019) Functional shifts in lake zooplankton communities with hypereutrophication. *Freshw. Biol.*, **64**, 608–616.
Moustaka-gouni, M. and Sommer, U. (2020) Effects of Harmful Blooms of Large-Sized and Colonial Cyanobacteria on Aquatic Food Webs. *Water*, **12**, 1–19.
Nimick, D. A. *et al.* (2011) Diel biogeochemical processes and their effect on the aqueous chemistry of streams: A review. *Chem. Geol.*, **283**, 3–17.
Oksanen, J. *et al.* (2020) vegan: Community Ecology Package.
Onandia, G. *et al.* (2015) Zooplankton grazing on natural algae and bacteria under hypertrophic conditions. *Limnetica*, **34**, 541–560.
den Oude, P. J. and Gulati, R. D. (1988) Phosphorus and nitrogen excretion rates of zooplankton from the eutrophic Loosdrecht lakes, with notes on other P sources for phytoplankton requirements. *Hydrobiologia*, **169**, 379–390.
Persson, J. *et al.* (2010) To be or not to be what you eat: Regulation of stoichiometric homeostasis among autotrophs and heterotrophs. *Oikos*, **119**, 741–751.
Prater, C. *et al.* (2017) Interactive effects of genotype and food quality on consumer growth rate and elemental content. *Ecology*, **98**, 1399–1408.
R Core Team (2021) R: A language and environment for statistical computing.
Rogers, T. *et al.* (2020) Trophic control changes with season and nutrient loading in lakes. *Ecol. Lett.*, **23**, 1287–1297.
Rönicke, H. *et al.* (2010) Changes of the plankton community composition during chemical neutralisation of the Bockwitz pit lake. *Limnologica*, **40**, 191–198.
Sarnelle, O. and Knapp, R. A. (2005) Nutrient recycling by fish versus zooplankton grazing as drivers of the trophic cascade in alpine lakes. *Limnol. Oceanogr.*, **50**, 2032–2042.

716 Schaffner, L. R. *et al.* (2019) Consumer-resource dynamics is an eco-evolutionary process in a
717 natural plankton community. *Nat. Ecol. Evol.*, **3**, 1351–1358.
718 Sharitt, C. A. *et al.* (2021) Nutrient excretion by fish supports a variable but significant
719 proportion of lake primary productivity over 15 years. *Ecology*, **0**, 1–8.
720 Shirokova, L. S. *et al.* (2020) Diel cycles of carbon, nutrient and metal in humic lakes of
721 permafrost peatlands. *Sci. Total Environ.*, **737**, 139671.
722 Sommer, U. *et al.* (2012) Beyond the Plankton Ecology Group (PEG) Model: Mechanisms
723 Driving Plankton Succession. *Annu. Rev. Ecol. Evol. Syst.*, **43**, 429–448.
724 Song, K. and Burgin, A. J. (2017) Perpetual Phosphorus Cycling: Eutrophication Amplifies
725 Biological Control on Internal Phosphorus Loading in Agricultural Reservoirs. *Ecosystems*,
726 **20**, 1483–1493.
727 Sournia, A. (1978) Phytoplankton Manual. *Monographs on Oceanographic Methodology*.
728 UNESCO, Paris.
729 Spooner, D. E. *et al.* (2013) Nutrient loading associated with agriculture land use dampens the
730 importance of consumer-mediated niche construction. *Ecol. Lett.*, **16**, 1115–1125.
731 Sterner, R. W. (1990) The Ratio of Nitrogen to Phosphorus Resupplied by Herbivores :
732 Zooplankton and the Algal Competitive Arena. *Am. Nat.*, **136**, 209–229.
733 Stoddard, J. L. *et al.* (2016) Continental-Scale Increase in Lake and Stream Phosphorus: Are
734 Oligotrophic Systems Disappearing in the United States? *Environ. Sci. Technol.*, **50**, 3409–
735 3415.
736 Striebel, M. *et al.* (2016) Phytoplankton responses to temperature increases are constrained by
737 abiotic conditions and community composition. *Oecologia*, **182**, 815–827.
738 Teurlincx, S. *et al.* (2017) Species sorting and stoichiometric plasticity control community C:P
739 ratio of first-order aquatic consumers. *Ecol. Lett.*, **20**, 751–760.
740 Vanni, M. J. (2002) Nutrient cycling by animals in freshwater ecosystems. *Annu. Rev. Ecol.*
741 *Syst.*, **33**, 341–370.
742 Vanni, M. J. *et al.* (2006) Nutrient cycling by fish supports relatively more primary production as
743 lake productivity increases. *Ecology*, **87**, 1696–1709.
744 Wang, M. *et al.* (2019) Seasonal Pattern of Nutrient Limitation in a Eutrophic Lake and
745 Quantitative Analysis of the Impacts from Internal Nutrient Cycling. *Environ. Sci. Technol.*,
746 **53**, 13675–13686.

747 Weber, M. J. and Brown, M. L. (2009) Effects of Common Carp on Aquatic Ecosystems 80
748 Years after “Carp as a Dominant”: Ecological Insights for Fisheries Management. *Rev.*
749 *Fish. Sci.*, **17**, 524–537.
750 Wentzky, V. C. *et al.* (2020) Seasonal succession of functional traits in phytoplankton
751 communities and their interaction with trophic state. *J. Ecol.*, **108**, 1649–1663.
752 Wilson, H. F. and Xenopoulos, M. A. (2011) Nutrient recycling by fish in streams along a
753 gradient of agricultural land use. *Glob. Chang. Biol.*, **17**, 130–139.
754 Zingel, P. *et al.* (2007) Ciliates are the dominant grazers on pico- and nanoplankton in a shallow,
755 naturally highly eutrophic lake. *Microb. Ecol.*, **53**, 134–142.
756

TABLE & FIGURE LEGENDS

Table 1. List of initial explanatory variables input to the distance based-Redundancy Analysis of phytoplankton community composition.

Table 2. Statistics for the distance based-Redundancy Analysis of phytoplankton community composition in Green Valley Lake from May to September 2019.

Figure 1. (A) Surface water nitrogen and (B) phosphorus concentrations split between total, dissolved inorganic, and zooplankton body storage over the course of the growing season. (C) surface water molar nitrogen: phosphorus (N:P) ratios split between total and inorganic pools with the dashed line denoting inferred nutrient limitation (Guildford and Hecky, 2000). (D) molar N:P ratios of the zooplankton community.

Figure 2. (A) Zooplankton biomass and community composition and (B) phytoplankton biomass and community composition over the course of the growing season in Green Valley Lake, IA.

Figure 3. The estimated concentration of total zooplankton community excretion produced over a day compared with the surface water dissolved (A) nitrogen and (B) phosphorus concentrations measured the same day as a percentage. Estimates of zooplankton excretion were derived from published allometric equations of zooplankton body size and excretion rate (Hébert, *et al.*, 2016). The dark lines represent the estimated excretion of either phosphorus or nitrogen, and the shaded area represents the error associated with the estimate for each sampling day.

Figure 4. (A) Density ridgeline plots of phytoplankton greatest axial distance (GALD, µm) and zooplankton body size (µm) over the course of the growing season in Green Valley Lake, IA. The black vertical line within each distribution represents the mean. (B) Mean difference between zooplankton length and phytoplankton GALD. DOYs that are missing either phytoplankton GALD or zooplankton length are the result of sample loss or no available data.

Figure 5. Distance based-Redundancy Analysis (db-RDA) of the phytoplankton community in Green Valley Lake from May to September 2019. Dots represent sampling points, and the

numbers 1-14 are DOY 143, 150, 164, 172, 178, 192, 199, 206, 211, 213, 220, 227, 245, 251, respectively. DOY 245 (13) was omitted from the diagram as there were no available data for inorganic N and P thus the data were omitted from the analysis. The significant explanatory variables are represented by black arrows.

TABLES

Table 1.

Explanatory Variable	Mean	Range
Zooplankton Biomass (µg L^{-1})	87.88	1.78 - 248.55
Zooplankton N:P Excretion	3.05	2.56 - 3.52
Zooplankton Community N:P	18.29	13.62 - 23.59
Dissolved Inorganic N (µM)	33.44	2.86 - 103.50
Temperature (°C)	87.88	1.78 - 248.55
pH	18.29	13.62 - 23.59

Table 2.

Permutation test variable	Sums of Squares	pseudo-*F*	*p*-value
Full model	1.27	2.68	**0.001**
First axis	0.86	3.62	**0.004**
Second axis	0.41	1.74	0.073
Inorganic N	0.47	2.00	**0.043**
Temperature (°C)	0.80	3.36	**0.003**
Residual	2.37		

812 **FIGURES**

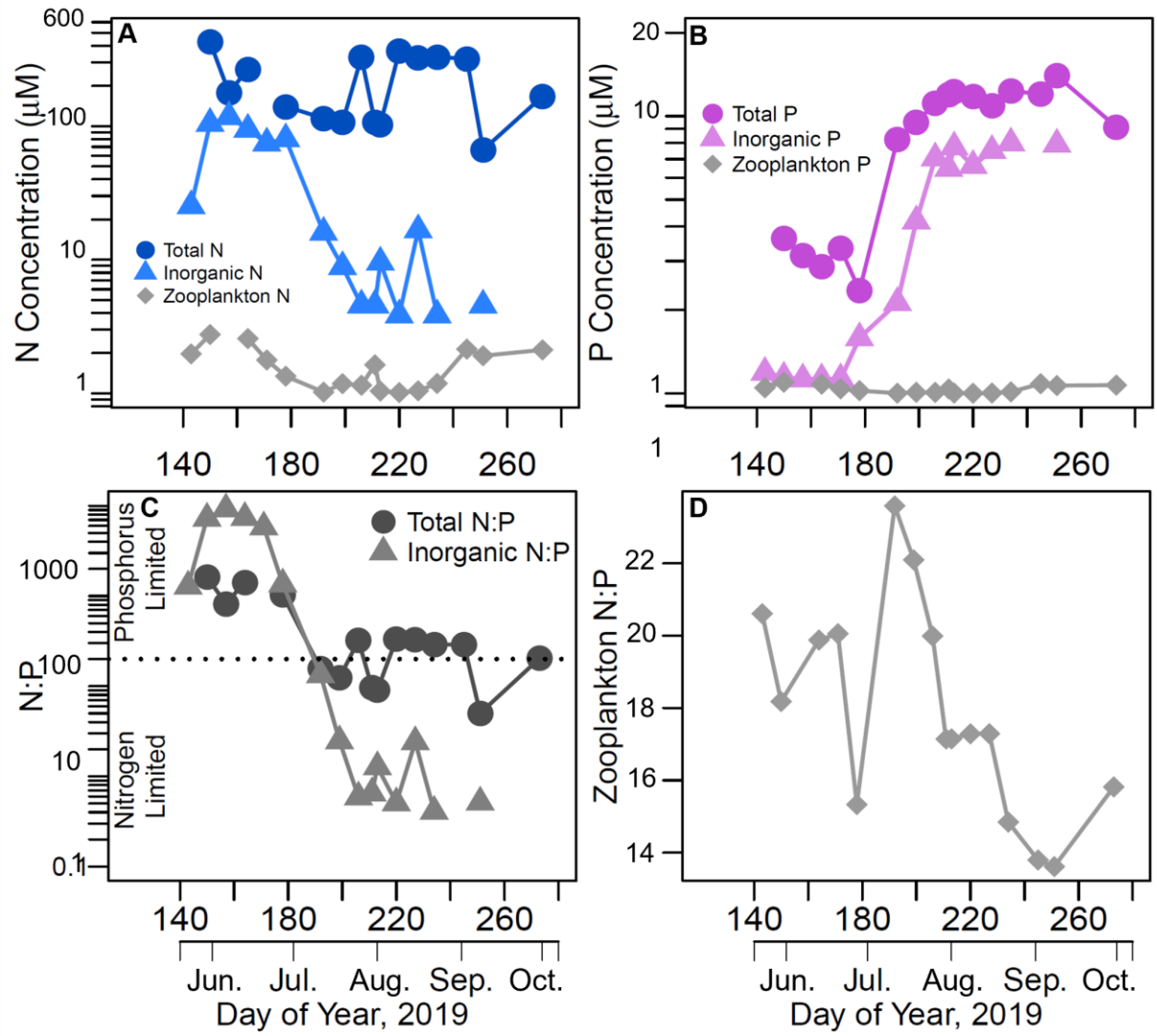

813

814 Figure 1.

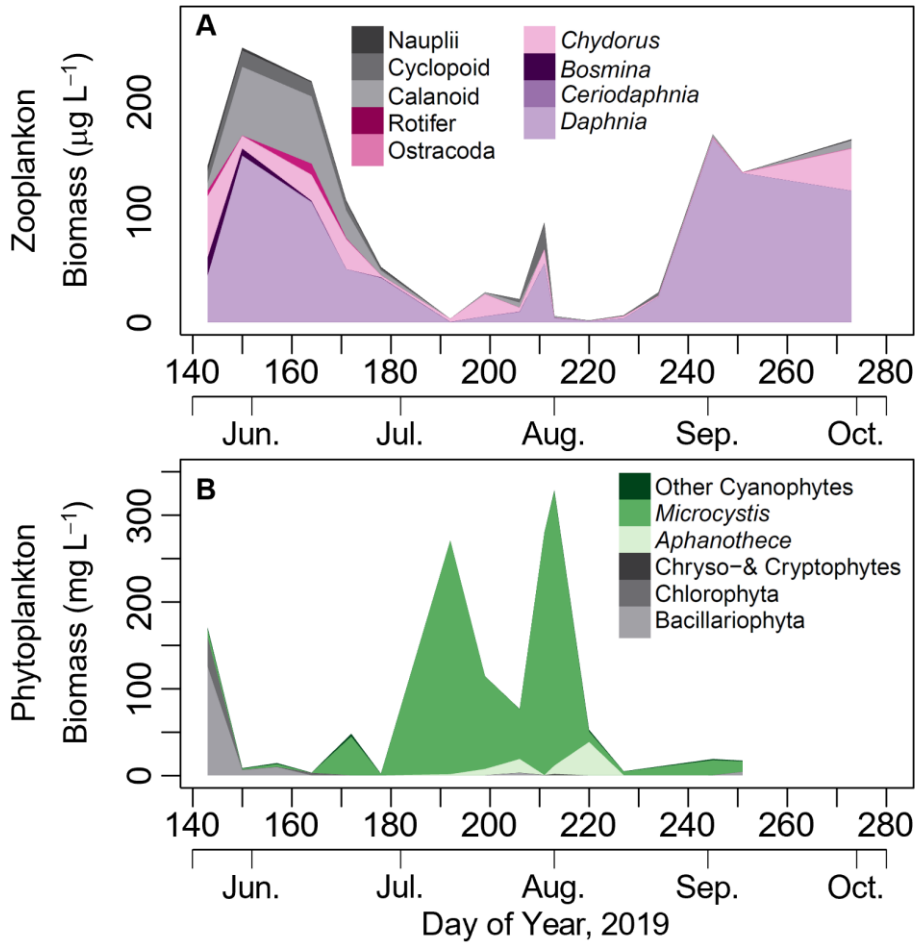

815

816 Figure 2.

817

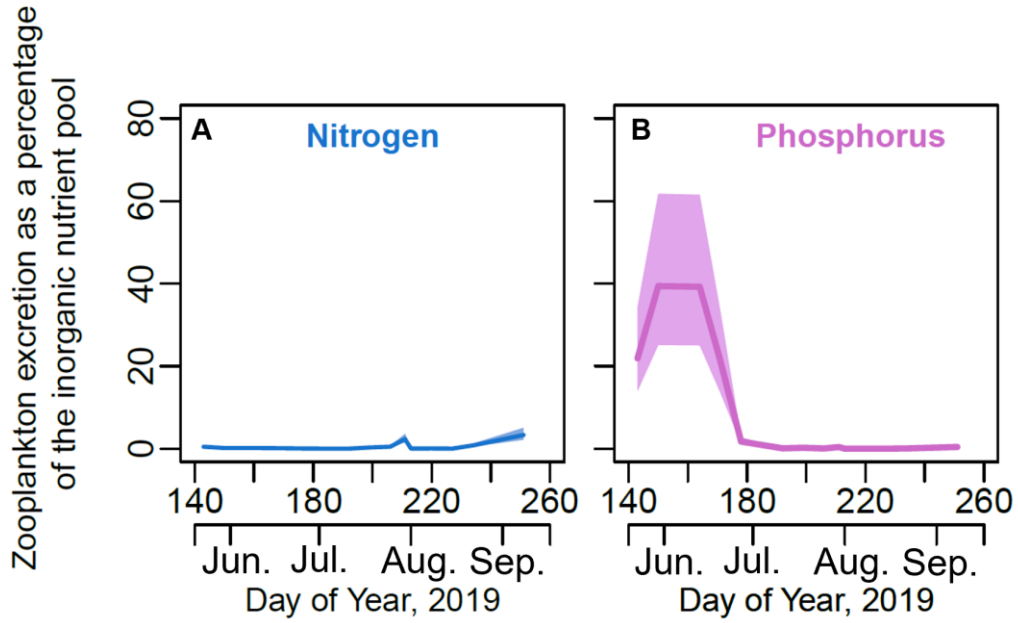

818

819 Figure 3.

820

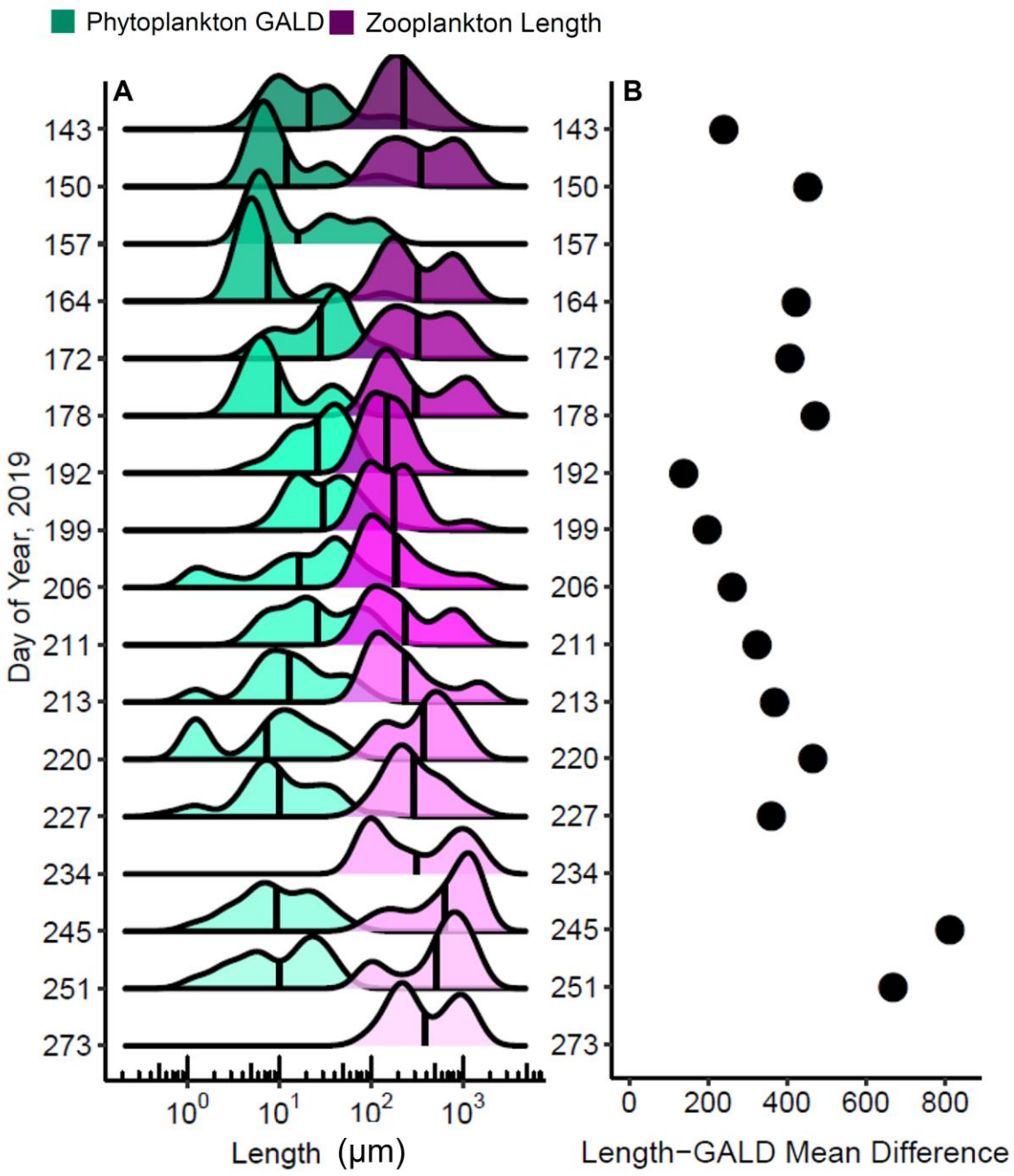

821
822 Figure 4.

823

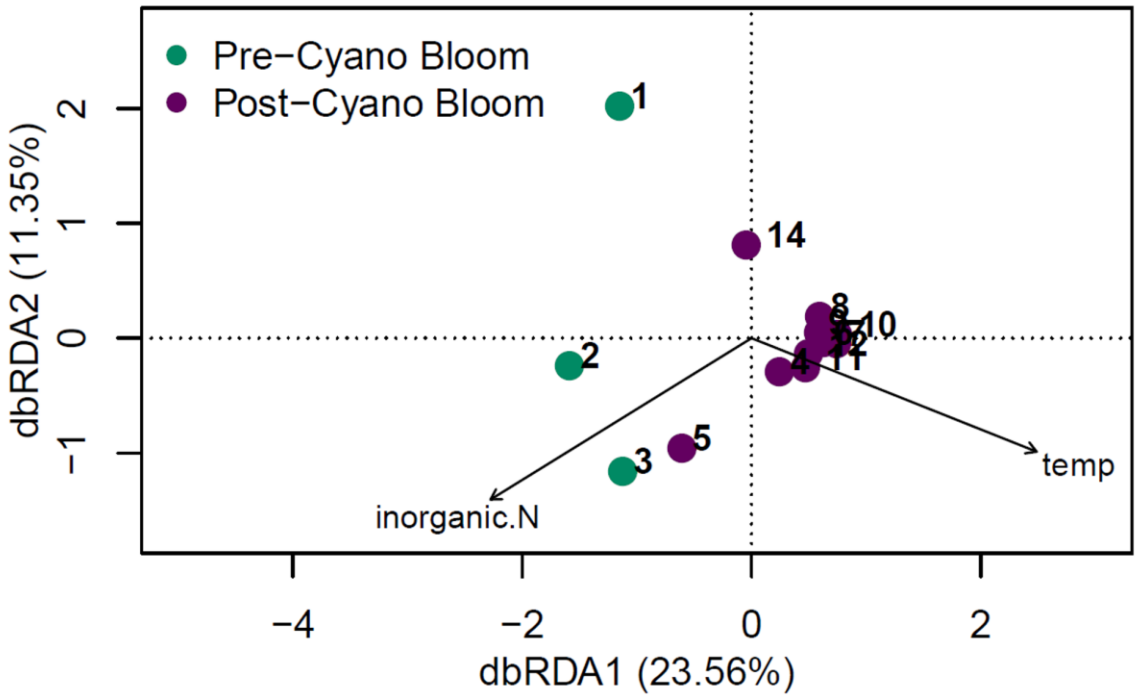

824

825 Figure 5.

826

Contribution of zooplankton nutrient recycling and effects on phytoplankton size structure in a hypereutrophic reservoir

Tyler J. Butts[1,3*], Eric K. Moody[2], Grace M. Wilkinson[1,3]

[1]Ecology, Evolution and Organismal Biology Department, Iowa State University, Ames, IA

[2]Department of Biology, Middlebury College, Middlebury, VT

[3]Current Address: Center for Limnology, University of Wisconsin – Madison, Madison, WI

***Corresponding Author:**

Tyler Butts

tjbutts@wisc.edu

Key Words: Nutrient cycling, stoichiometry, hypereutrophic, body size

Supplementary Material

Nutrient concentrations and speciation

The following equations describe how we defined the major fractions of nitrogen (N) and phosphorus (P) in Green Valley Lake. Total N in freshwater is composed organic and inorganic fractions:

$$TN = orgN + DIN \quad (1)$$

where *TN* is total N, *orgN* is organic N in both the particulate (organisms and detritus) and dissolved (urea) form, and *DIN* is dissolved inorganic N composed of *NOx* and *NHx* representing nitrate + nitrite and ammonium + ammonia, respectively. Previous data from the last decade in Green Valley Lake indicated *NHx* were extremely low or undetectable in the surface waters during the summer months. If we assume that *NHx* is undetectable (1) simplifies to:

$$TN = orgN + NOx \quad (2)$$

allowing calculation of *orgN* by rearranging (2):

$$orgN = TN - NOx \quad (3)$$

Thus, we could characterize N pools as total (*TN*) representing dissolved and particulate forms of N, organic (*orgN*) representing dissolved organic N (urea) and seston, and inorganic N (*NOx)* representing *DIN* in the surface waters. For our analyses we focused on the TN and DIN pools.

Similarly, P is composed of organic and inorganic fractions in reservoir surface waters:

$$TP = POP + PIP + DIP + DOP \quad (4)$$

where *TP* is total P, *POP* is particulate organic P, *PIP* is particulate inorganic P, *DIP* is dissolved inorganic P, and *DOP* is dissolved organic P. *DIP* and *PIP* were both present within the water column, but our focus for this study was on *DIP* which is far more bioavailable to phytoplankton than *PIP* (Zhou *et al.*, 2005) and thus more influential to nutrient cycling via zooplankton-phytoplankton interactions. Previous data from the last decade in Green Valley Lake indicated *PIP* was extremely low or undetectable in the surface waters during the summer months. Thus, (4) can be simplified by combining *DOP* and *POP* to one organic pool (*orgP*) and using *SRP* as a measure of *DIP* over the course of the growing season:

$$TP = orgP + SRP \quad (5)$$

Therefore, we could characterize P pools as total (*TP*) representing dissolved and particulate forms of P, organic (*orgP*) representing dissolved organic P and seston, and inorganic (*SRP*) representing *DIP* in the surface waters. For our analyses we focused on the TP and SRP pools.

Ammonium + ammonia (NHx) (EPA method 103-A v6) and inorganic suspended solids were measured at the same location in the lake three times during the summer by the Iowa Ambient Lakes Monitoring program (IDNR 2021)**.** Ammonium was analyzed through the alkaline phenate method on a Seal Analytical AQ2 Discrete Analyzer and inorganic particulates were determined via difference between total and volatile suspended solids (USGS method I-3765-85).

Zooplankton excretion equations

Individual zooplankton excretion of P was determined using the following equation from Hébert *et al.*, (2016):

$$ln\left(P_{exc,h}\right) = 0.56 + \left(0.70ln(Z_{BS})\right) \quad (6)$$

where $P_{exc,h}$ is excreted P (nM of P individual^{-1} hour^{-1}) and Z_{BS} is the dry mass of an individual zooplankter (mg). Zooplankton excretion of N was determined in a similar manner:

$$ln\left(N_{exc,h}\right) = 2.50 + \left(0.84ln(Z_{BS})\right) \quad (7)$$

where $N_{exc,h}$ is excreted N (nM of N individual^{-1} hour^{-1}).

Data were then converted to µM of N or P per day using the following conversions:

$$\frac{nmol\ N\ or\ P}{individual\ \cdot hour} \cdot \frac{24\ hours}{1\ day} \cdot \frac{individuals}{L} \cdot \frac{1\ \mu mol}{1000\ nmol} = \frac{\mu M\ N\ or\ P}{day} \quad (8)$$

The allometric equations were derived from a combined dataset of marine and freshwater zooplankton. Using only the freshwater data did not significantly change the slope, nor was the relationship between excretion and body size significant due to the much smaller sample size. Thus, we only present the combined freshwater and marine model as presented in Hébert *et al.* (2016). Additionally, we used zooplankton excretion equations from Wen and Peters (1994). Specifically, we used their multivariate regression equations for crustacean zooplankton which corrected for temperature (K) and experimental duration (h) in their estimates of excretion. As

our data did not have an experimental duration, we dropped the experimental duration correction resulting in the following equations:

$$Log_{10}(P_{exc,wp}) = -5.28 + (0.61 * log_{10}(Z_{BS})) + (0.01 * T) \quad (9)$$

Where $P_{exc,wp}$ is excreted P (µg d^{-1}), Z_{BS} is the body size of an individual zooplankter (µg), and T is water temperature (K).Similarly, for N excretion:

$$Log_{10}(N_{exc,wp}) = -3.47 + (0.74 * log_{10}(Z_{BS})) + (0.00002 * T^2) \quad (10)$$

Where $N_{exc,wp}$ is excreted N (µg d^{-1}), Z_{BS} is the body size of an individual zooplankter (µg), and T is water temperature (K). The pattern of zooplankton excretion was consistent between the two methods; however, the magnitude of excretion was different (Supplementary Table S3).

Zooplankton Food Size Range

We collected data on the reported food size range of *Bosmina*, *Ceriodaphnia*, *Chydorus*, *Daphnia*, *Diaphanosoma*, Cyclopoida, Calanoida, Rotifera, and nauplii from the literature (Sweeney *et al.*, 2022; Helenius and Saiz, 2017; Barnett *et al.*, 2007). If a species primarily fed on zooplankton rather than phytoplankton, they were not included within our trait data. We did not find appropriate food size range data for Ostracods and thus they were removed from our analysis. If there were multiple size ranges reported for different species within a larger taxonomic group (e.g., *Daphnia*) we calculated the mean of the minimum food size range and maximum food size range (Supplementary Table S5).

Supplementary References

Barnett, A. J. *et al.* (2007) Functional diversity of crustacean zooplankton communities : towards a trait-based classification. 796–813.

Havens, K. E. and Beaver, J. R. (2013) Zooplankton to phytoplankton biomass ratios in shallow Florida lakes: An evaluation of seasonality and hypotheses about factors controlling variability. *Hydrobiologia*, **703**, 177–187.

Hébert, M. P. *et al.* (2016) A meta-analysis of zooplankton functional traits influencing ecosystem function. *Ecology*, **97**, 1069–1080.

Helenius, L. K. and Saiz, E. (2017) Feeding behaviour of the nauplii of the marine calanoid copepod Paracartia grani Sars: Functional response, prey size spectrum, and effects of the presence of alternative prey. *PLoS One*, **12**, 1–20.

Iowa Department of Natural Resources (IDNR) (2021) Water Quality Monitoring and Assessment Section. AQuIA [database].

Leroux, S. and Loreau, M. (2015) Theoretical perspectives on bottom-up and top-down interactions across ecosystems. In Hanley, T. and La Pierre, K. (eds), *Trophic Ecology: Bottom-up and top-down interactions across aquatic and terrestrial systems*. Cambridge University Press, pp. 3–27.

Sweeney, K. *et al.* (2022) Grazing impacts of rotifer zooplankton on a cyanobacteria bloom in a shallow temperate lake (Vancouver Lake , WA ,. *Hydrobiologia*.

Wen, Y. H. and Peters, R. H. (1994) Empirical models of phosphorus and nitrogen excretion rates by zooplankton. *Limnol. Oceanogr.*, **39**, 1669–1679.

Zhou, A. *et al.* (2005) Phosphorus adsorption on natural sediments: Modeling and effects of pH and sediment composition. *Water Res.*, **39**, 1245–1254.

Supplementary Table and Figure Legends

Supplementary Table S1. Zooplankton genera, order, or class identified over the course of the growing season in Green Valley Lake.

Supplementary Table S2. Phytoplankton genera identified over the course of the growing season in Green Valley Lake.

Supplementary Table S3. Estimated zooplankton excretion of N and P (μM d^{-1}) using different published allometric equations from Hébert *et al.* (2016) and Wen and Peters (1994). Uncertainty estimates derived from the allometric equation parameters in Hébert *et al.* (2016) are presented in parentheses.

Supplementary Table S4. Zooplankton taxa food size range data collected from the literature. Minimum food size range (Min FSR (μm)) and maximum food size range (Max FSR (μm)) represent either a single species or an average of multiple species. When an average was taken, the standard deviation is presented.

Supplementary Table S5. Potential zooplankton nutrient turnover of soluble reactive phosphorus in Green Valley Lake. Values represent the number of days it would take zooplankton excretion alone to replenish the water column concentration of dissolved inorganic phosphorus on a given sampling day. Missing values were the result of sample loss or the lack of available data and are denoted by NA.

Supplementary Figure S1. Historical water quality and plankton data for Green Valley Lake. The different colors represent before or after the clear-water period which we determined was around DOY 170 using a breakpoint analysis for the period 2011 – 2019. Dark color and square shape denote data before DOY 170, and light color and circle shape denote data post DOY 170. From left to right, top to bottom the variables represented are total nitrogen, nitrate, ammonium, total phosphorus, soluble reactive phosphorus, inorganic particulates, zooplankton biomass, non-Cyanophyta biomass, and Cyanophyta biomass. Data were collated from the Ambient Lakes Monitoring program in the state of Iowa (IDNR, 2021).

Supplementary Figure S2. The estimated zooplankton excretion nitrogen: phosphorus ratio derived from published allometric equations of zooplankton body size and excretion rate (Hébert *et al.*, 2016).

Supplementary Figure S3. The ratio of zooplankton: phytoplankton biomass across the summer growing season in Green Valley Lake. The dashed lines represent the threshold for either weak (~10%) or strong (~40-50%) top-down control on phytoplankton biomass (Leroux and Loreau, 2015; Havens and Beaver, 2013).

Supplementary Figure S4. The percentage of individual phytoplankton GALD measurements per sampling date that fell within the zooplankton community food size range calculated for the same sampling date. Dark bars represent the percentage of phytoplankton GALD measurements that fell within the zooplankton food size range and light bars represent the percentage that fell outside of that range.

Supplementary Figure S5. Density ridgeline plots of phytoplankton greatest axial distance (GALD, µm) and zooplankton body mass (µg) over the course of the growing season in Green Valley Lake, IA. The black vertical line within each distribution represents the mean. DOYs that are missing either phytoplankton GALD or zooplankton length are the result of sample loss or no available data.

Supplementary Figure S6. Pearson correlations of (A) zooplankton body length (µm) and (B) zooplankton body mass (µg) by phytoplankton greatest axial linear distance (GALD, µm).

968 *Tables*

969 Supplementary Table S1.

Taxonomic Group	Taxa identified in Green Valley Lake included in grouping
Large Cladocera	*Daphnia* *Simocephalus* *Ceriodaphnia*
Small Cladocera	*Bosmina* *Chydorus*
Ostracod	Ostracoda
Calanoids	Calanoida
Cyclopoids	Cyclopoida
Nauplii	Copepod nauplii
Rotifers	*Asplanchna* *Keratella cochlearis* *Keratella quadrata* *Pompholyx* *Trichocerca* *Filinia*

970

971 Supplementary Table S2.

Taxonomic Group	Taxa identified in Green Valley Lake included in grouping
Bacillariophyta	*Asterionella*
	Fragilaria
	Stephanodiscus
	Unknown pennate bacillariophyte
	Unknown centric bacillariophyte
Chlorophyta	*Chalmydomonas*
	Coelastrum
	Cosmarium
	Desmodesmus
	Elakatothrix
	Eudorina
	Monoraphidium
	Oocystis
	Pediastrum
	Schroederia
	Staurastrum
	Unknown chlorophyte
Chyrso - & Cryptophytes	*Mallomonas*
	Cryptomonas
	Komma
Aphanothece (Cyanophyte)	*Aphanothece*
Microcystis (Cyanophyte)	*Microcystis*
	Microcystis (Single-celled)
Other Cyanophytes	*Aphanizomenon*
	Aphanocapsa
	Merismopedia
	Planktolyngbya
	Pseudanabaena
	Snowella
	Woronichinia
	Dolichospermum

972

973 Supplementary Table S3.

Zooplankton Excretion (μM N or P day^{-1})

	Nitrogen Excretion		**Phosphorus Excretion**	
DOY	Hébert	Wen & Peters	Hébert	Wen & Peters
143	0.159 (0.143- 0.242)	0.073	0.062 (0.040-0.100)	0.080
150	0.177 (0.116-0.270)	0.082	0.056 (0.036-0.088)	0.072
164	0.167 (0.110-0.255)	0.083	0.058 (0.037-0.091)	0.081
171	0.087 (0.057-0.133)	0.039	0.029 (0.018-0.045)	0.036
178	0.034 (0.022-0.051)	0.014	0.010 (0.007-0.016)	0.012
192	0.003 (0.002-0.004)	0.002	0.001 (0.001-0.002)	0.002
199	0.022 (0.014-0.033)	0.012	0.008 (0.005-0.012)	0.011
206	0.015 (0.010-0.022)	0.007	0.005 (0.003-0.007)	0.006
211	0.068 (0.045-0.104)	0.035	0.023 (0.014-0.035)	0.032
213	0.004 (0.002-0.005)	0.002	0.001 (0.001-0.007)	0.001
220	0.001 (0.001-0.002)	0.001	0.000 (0.000-0.002)	0.001
227	0.005 (0.003-0.007)	0.002	0.002 (0.001-0.003)	0.002
234	0.018 (0.012-0.027)	0.008	0.005 (0.003-0.008)	0.007
245	0.109 (0.072-0.167)	0.046	0.031 (0.020-0.049)	0.037
251	0.095 (0.062-0.145)	0.042	0.029 (0.019-0.046)	0.036
273	0.120 (0.079-0.183)	0.051	0.039 (0.025-0.061)	0.046

974

975 Supplementary Table S4.

Taxa	Min FSR (µm)	Standard Deviation	Max FSR (µm)	Standard Deviation	Source
Bosmina	1.4	NA	5	NA	Barnett et al. 2007
Ceriodaphnia	0.4	NA	7	NA	Barnett et al. 2007
Chydorus	0.4	NA	2	NA	Barnett et al. 2007
Daphnia	1.1	0.5	30	10	Barnett et al. 2007
Diaphanosoma	0.25	NA	5	NA	Barnett et al. 2007
Cyclopoida	6.9	6.1	54.2	43.5	Barnett et al. 2007
Calanoida	9.4	11.6	64	23	Barnett et al. 2007
Nauplii	4.5	NA	19.8	NA	Helenius & Saiz 2017
Rotifera	0	NA	75	NA	Sweeney et al. 2022

976

977 Supplementary Table S5.

Nutrient Pool	***DOY 143***	***DOY 150***	***DOY 164***	***DOY 172***	***DOY 178***	***DOY 192 - 273***
Soluble Phosphorus	5 d	3 d	3 d	5 d	57 d	>200 d

978

979

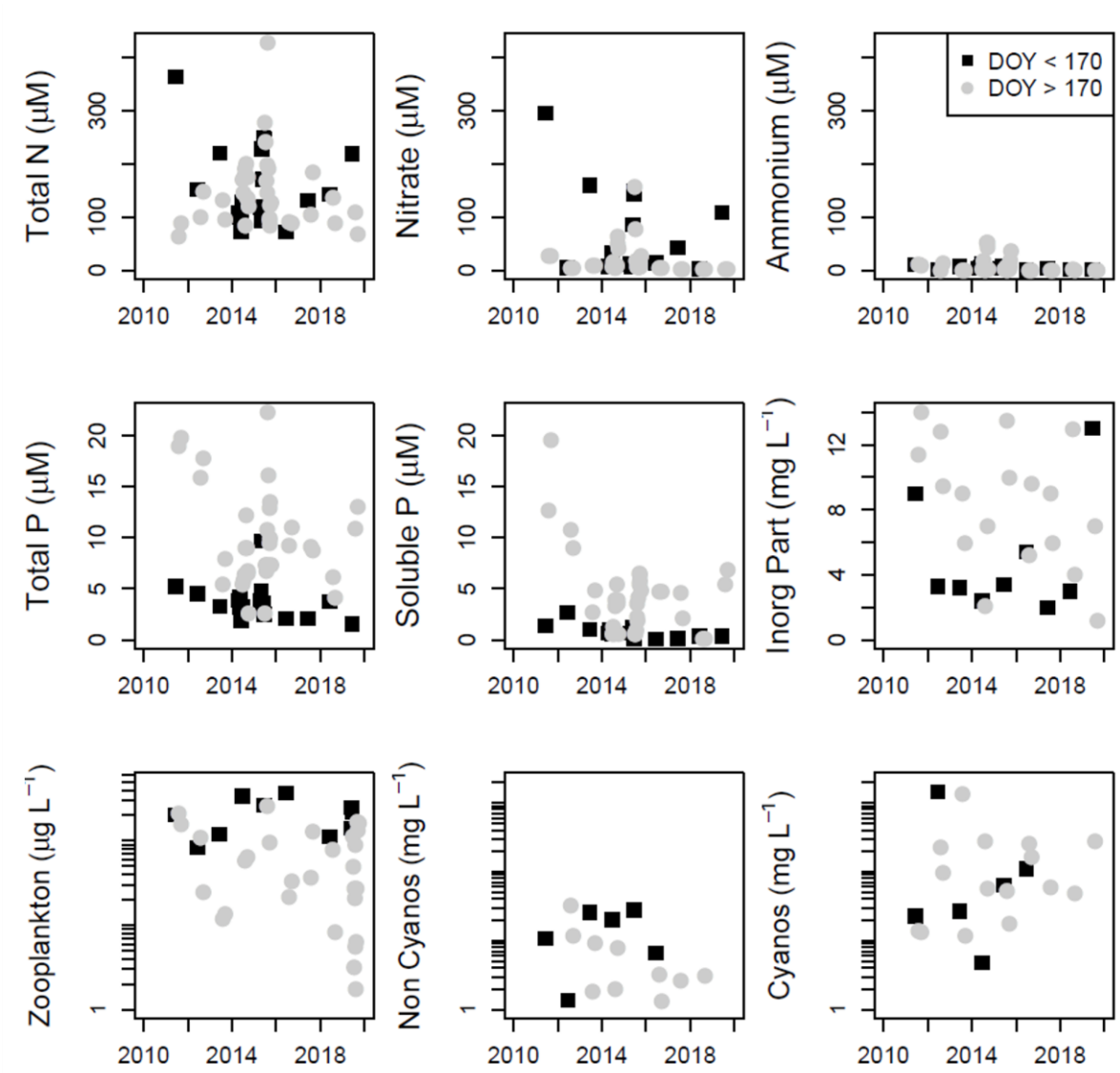

Supplementary Figure S1

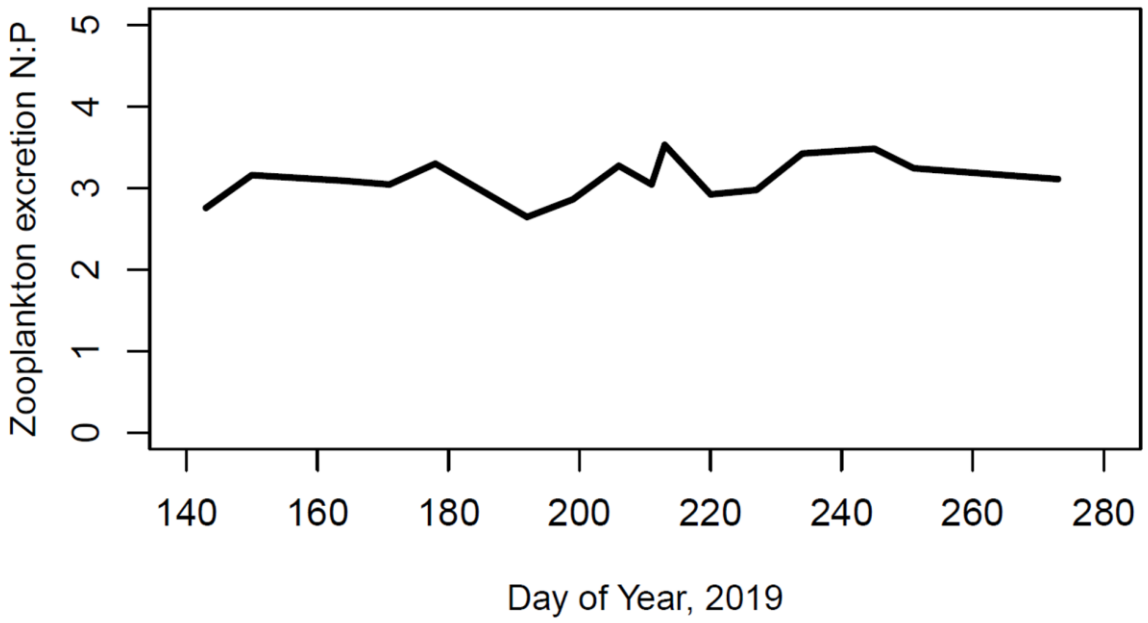

983

984 Supplementary Figure S2

985

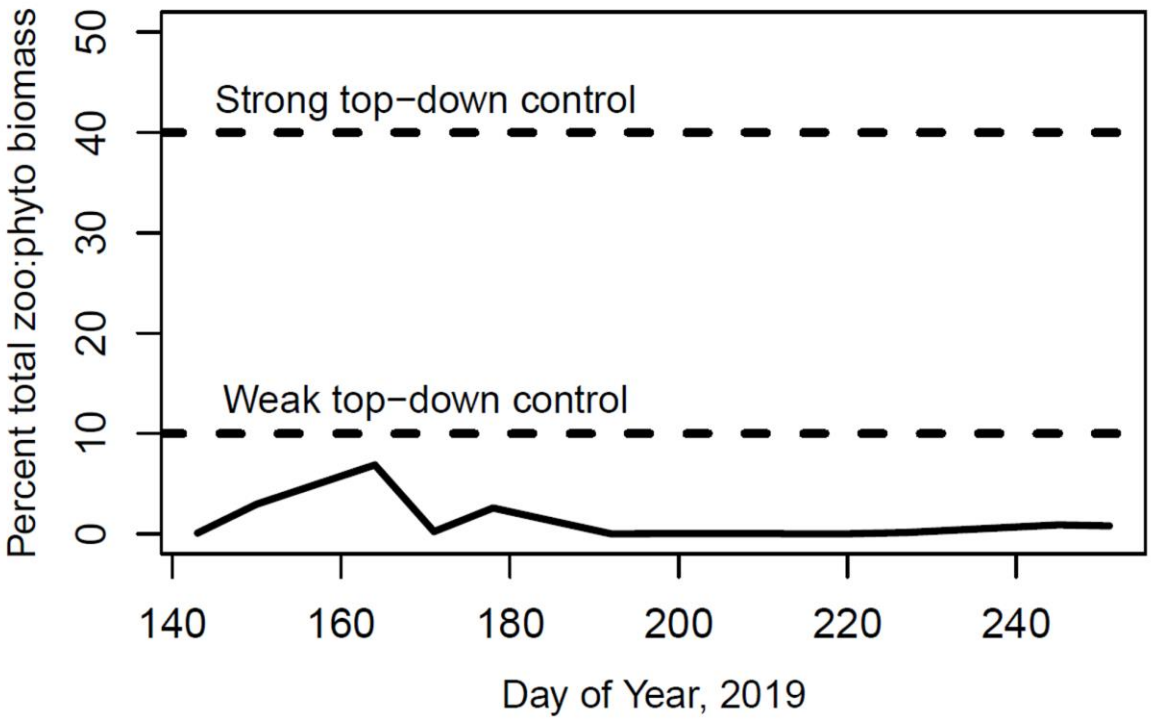

Supplementary Figure S3

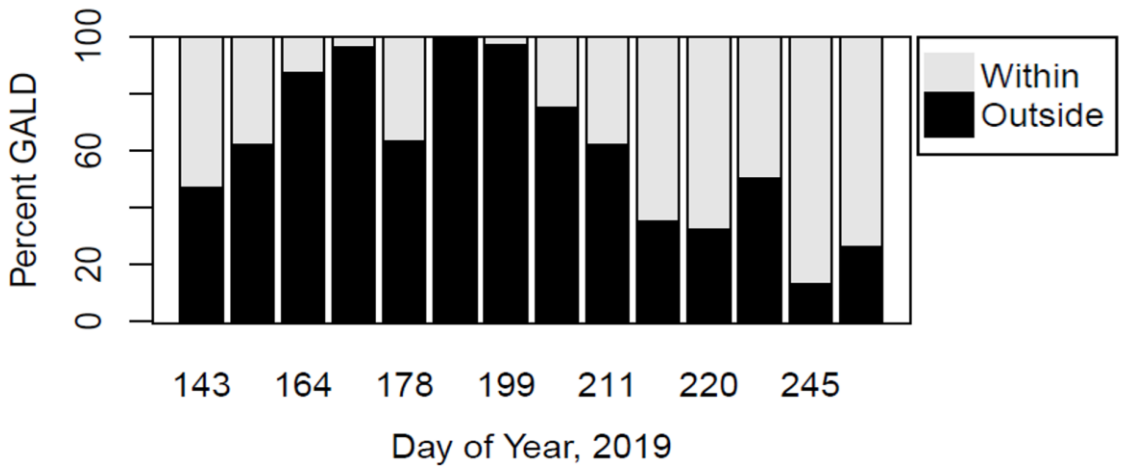

989

990 Supplementary Figure S4

991

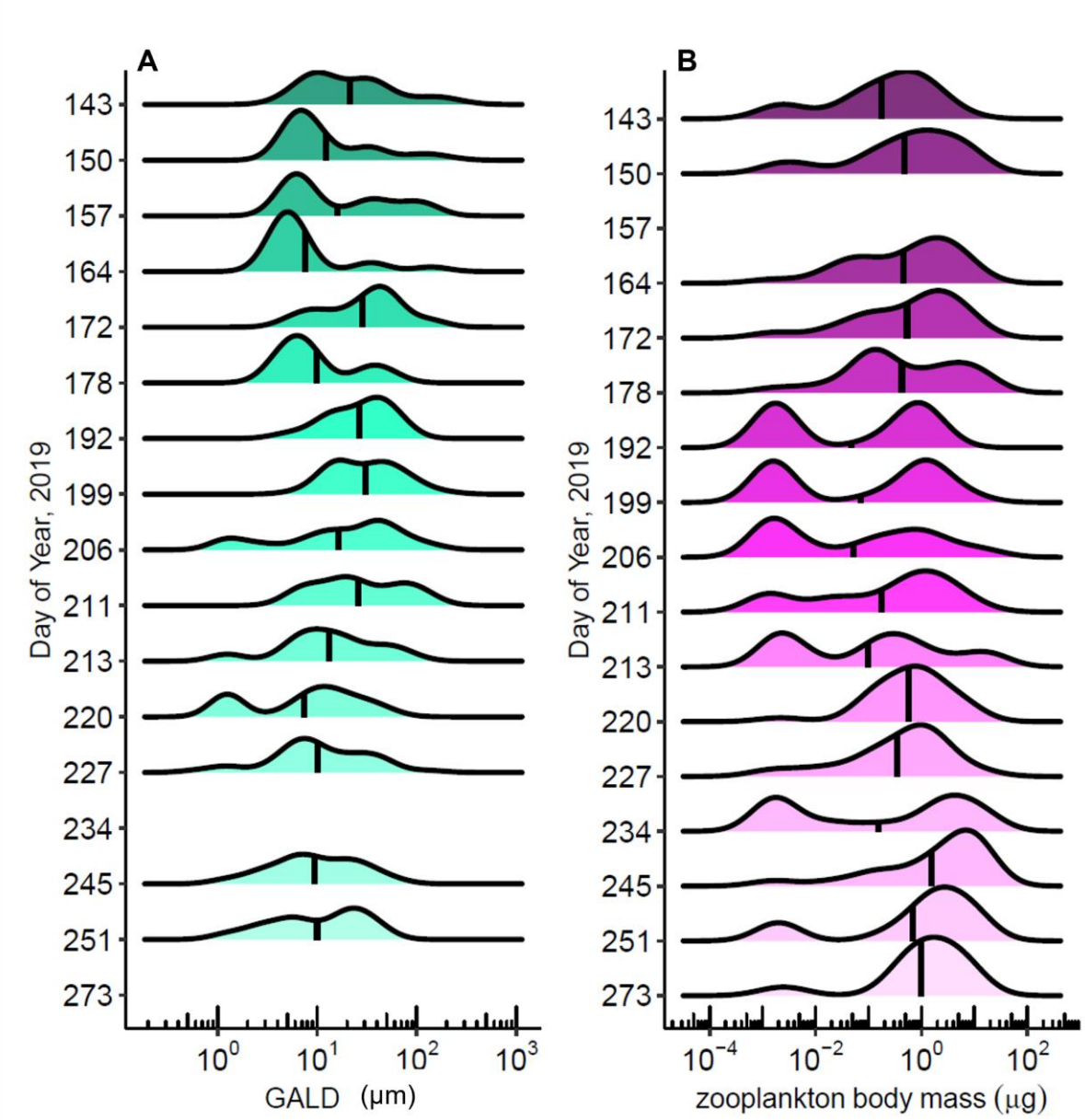

992

993 Supplementary Figure S5

994

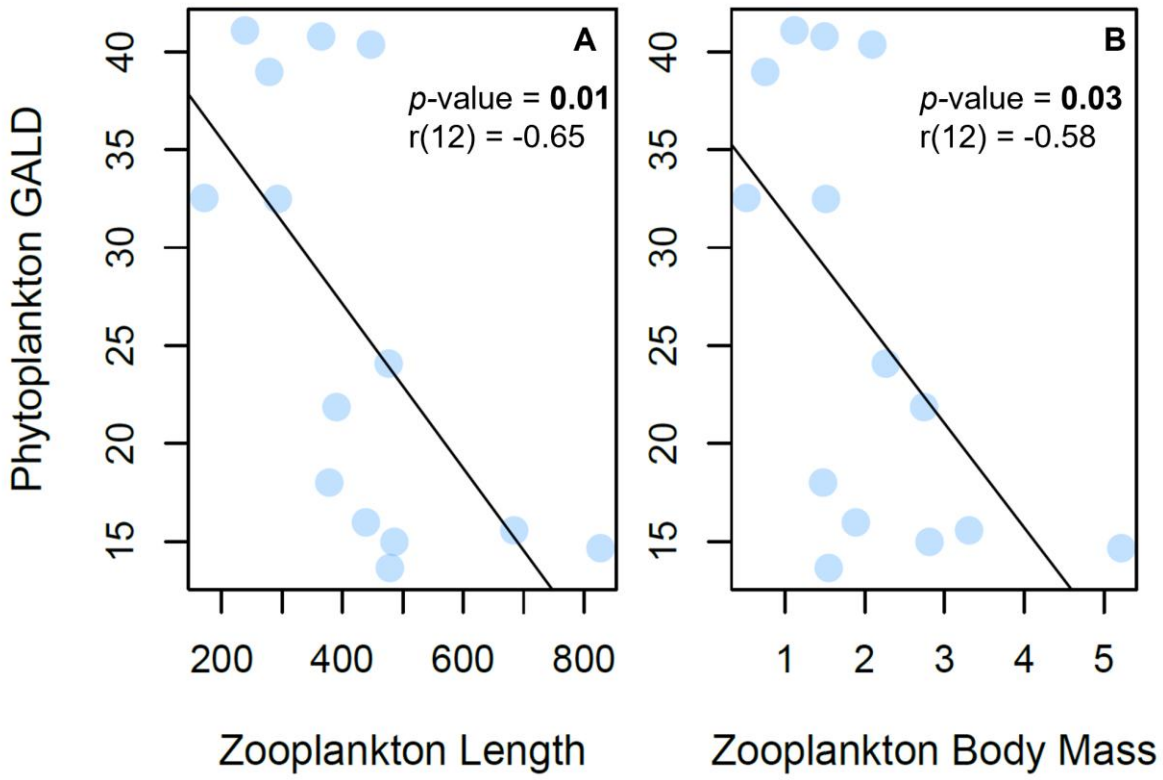

995

996 Supplementary Figure S6